Thermal Conductivity of Aqueous $Sr(NO_3)_2$ and $LiNO_3$ Solutions at High Temperatures and High Pressures

Ilmutdin M. Abdulagatov,*,†,§ Lala A. Akhmedova-Azizova,‡ and Nazim D. Azizov‡

Institute for Geothermal Problems, Dagestan Scientific Center, Russian Academy of Sciences, 367003 Shamilya Str. 39-A, Makhachkala, Dagestan, Russia, and Azerbaijan State Oil Academy, Baku, 370601, Azerbaijan

Thermal conductivity of five aqueous $Sr(NO_3)_2$ solutions of molality (0.249, 0.525, 1.181, 2.025, and 3.150) mol·kg^{-1} and four aqueous $LiNO_3$ solutions of molality (1.0, 1.7, 2.8, and 3.9) mol·kg^{-1} have been measured with a concentric-cylinder (steady) technique. Measurements were made at five isobars (0.1, 10, 20, 30, and 40) MPa for H_2O+$Sr(NO_3)_2$ and at four isobars (0.1, 10, 20, and 30) MPa for H_2O+$LiNO_3$ solutions. The range of temperature was (293.15 to 591.06) K. The total uncertainty of thermal conductivity, pressure, temperature, and molality measurements were estimated to be less than 2%, 0.05%, 30 mK, and 0.02%, respectively. The measured values of thermal conductivity were compared with data and correlations reported in the literature. The reliability and accuracy of the experimental method was confirmed with measurements on pure water, toluene, and H_2O + NaCl with well-known thermal conductivity values. The experimental and calculated values of thermal conductivity for pure water from IAPWS formulation show excellent agreement within their experimental uncertainties (AAD within 0.44%) in the temperature range from (308.4 to 704.2) K and at pressures up to 60 MPa. Correlation equations for thermal conductivity of the solutions studied were obtained as a function of temperature, pressure, and composition by a least-squares method from the experimental data. The AAD between measured and calculated values from this correlation equation for the thermal conductivity was (0.5 to 0.7) %.

Introduction

Transport properties of aqueous solutions are needed in many industrial and scientific applications such as calculation of design parameters, developments and utilization of geothermal and ocean thermal energy, efficient operation of high-temperature energy-generating systems, geology and mineralogy, for hydrothermal synthesis, biological processes of living organisms, and in prediction of heat- and mass-transfer coefficients under both laminar and turbulent regimes. Thermal conductivity data are required also for calculating flow and heat- and mass-transfer rates in various pieces of industrial equipment. To understand and control those processes that used electrolyte solutions, it is necessary to know their thermodynamic and transport properties. Because of lack of reliable experimental information on thermal conductivity of aqueous solutions, the design parameters are often obtained empirically.

A database of thermal conductivity in high-temperature aqueous systems is needed to support the advancement of theoretical work. Because of the complexity of the aqueous solutions, there are neither experimental data on representative systems nor predictive theoretical models available that will offer sufficient insight for an optimum process design. Currently available models still cannot treat real system as they are met in practice (for example, complex ionic solutions are extremely difficult). Better predictive models should be developed on basis reliable experimental information on thermodynamic and transport properties data. However, measurements of the thermal conductivity of aqueous salt solutions have so far been limited to rather narrow ranges of temperature, pressure, and concentration with less satisfactory accuracy.

Only limited experimental thermal-conductivity data of H_2O + $Sr(NO_3)_2$ and H_2O + $LiNO_3$ solutions over a wide range of temperatures, pressures, and compositions are available in the literature. For example, there are no measurements of thermal conductivity of aqueous $LiNO_3$ solutions at high pressures. Therefore, there is a sustained demand for new reliable thermal conductivity data of H_2O + $Sr(NO_3)_2$ and H_2O + $LiNO_3$ solutions, which cover wide temperature, pressure, and concentration ranges.

The main objective of the paper is to provide new accurate experimental thermal conductivity data for aqueous $Sr(NO_3)_2$ and $LiNO_3$ solutions at high temperatures (up to 591.06 K) and high pressures (up to 40 MPa). This work is a part of a continuing program on the transport properties of electrolytes in aqueous solutions. In previous studies,[1−13] we measured the thermal conductivity of 25 aqueous salt solutions at high temperatures (up to 573.15 K) and high pressures (up to 100 MPa). Thermal conductivity for aqueous $LiNO_3$ solutions has been previously studied only at atmospheric pressure and over narrow temperature (up to 373.15 K) and composition (up to 40 mass %) ranges.[14] Some of the reported thermal conductivities are inaccurate and inconsistent.

Abdulagatov and Magomedov[4] reported thermal conductivity data for H_2O + $Sr(NO_3)_2$ solutions at pressures from (0.1 to 100) MPa at temperatures from (293.15 to 473.15) K and at compositions between (2.5 and 20.0) mass %.

* To whom correspondence should be addressed. E-mail: ilmutdin@boulder.nist.gov.
† Russian Academy of Sciences.
‡ Azerbaijan State Oil Academy.
§ Present address: Physical and Chemical Properties Division, National Institute of Standards and Technology, 325 Broadway, Boulder, Colorado 80305.

10.1021/je0342466 CCC: $27.50 © 2004 American Chemical Society
Published on Web 04/06/2004

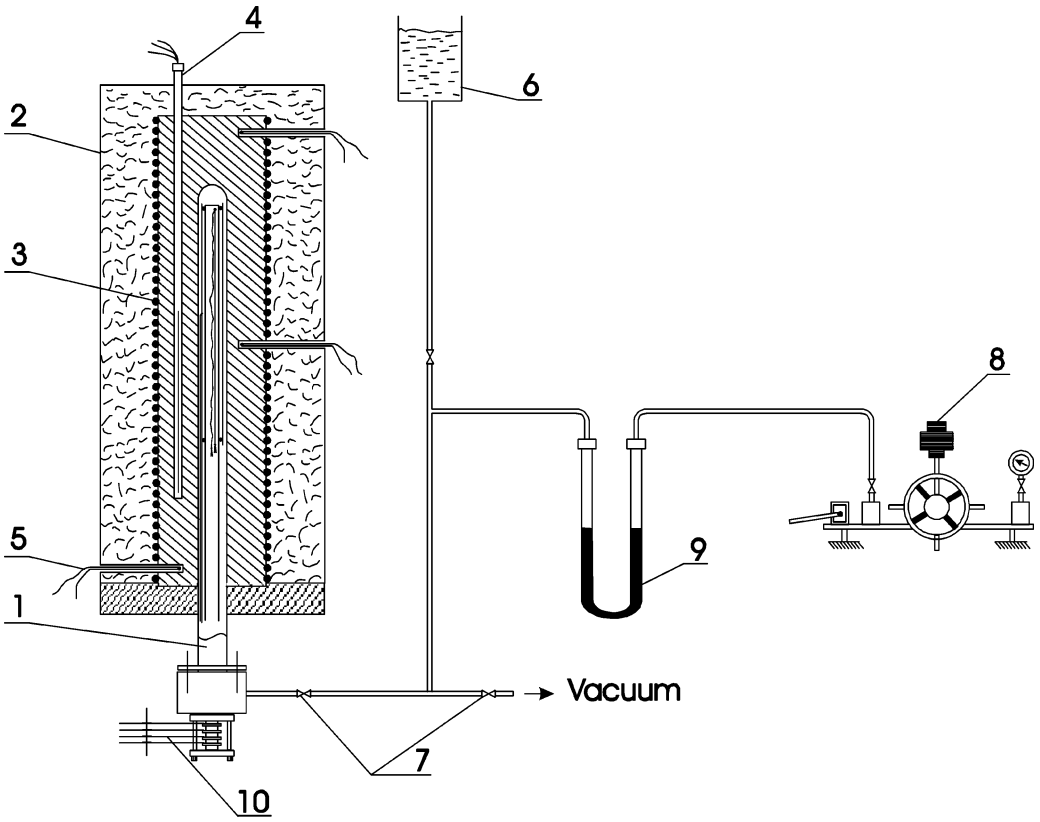

Figure 1. Schematic diagram of the experimental apparatus for measuring the thermal conductivity of liquids and liquid mixtures at high temperatures and high pressures by the coaxial cylinders method. 1, High-pressure autoclave; 2, thermostat; 3, heater; 4, PRT; 5, thermocouple; 6, filling tank; 7, set of valves; 8, dead-weight pressure gauge (MP-600); 9, separating U-shape capillary tube; 10, electrical feedthrough.

Measurements were made by means of the parallel plate technique. The uncertainty in the thermal conductivity measurements was about 1.6%. The results of measurements were represented by correlation equation

$$\lambda_{sol}(T,P,\omega) = \lambda_{H_2O}(P,T)[1 - B(\omega + (2 \times 10^{-4})\omega^3)] - (2 \times 10^{-8})PT\omega \quad (1)$$

$$\lambda_{H_2O}(P,T) = (7 \times 10^{-9})T^3 - (1.511 \times 10^{-5})T^2 + (8.802 \times 10^{-3})T - 0.8624 + (1.6 \times 10^{-6})PT$$

where $\lambda_{sol}(T,P,x)$ is the thermal conductivity of solution in $W \cdot m^{-1} \cdot K^{-1}$, $\lambda_{H_2O}(P,T)$ is the thermal conductivity of pure water in $W \cdot m^{-1} \cdot K^{-1}$, ω is the concentration in mass %, T is the temperature in K, P is pressure in MPa, and B is the adjusting parameter. The values of coefficient B in eq 1 for $H_2O + Sr(NO_3)_2$ and $H_2O + LiNO_3$ solutions are 0.00163 and 0.00274, respectively.[15] In the limit $\omega \rightarrow 0$, the thermal conductivity of pure water $\lambda_{H_2O}(P,T)$ is obtained from eq 1. Equation 1 is applicable in the temperature range from (273 to 473) K, pressures from (0.1 to 100) MPa, and concentrations between (0 and 25) mass %, although some reasonable extrapolation to high concentrations is possible.

Experimental Apparatus and Procedures

Apparatus and Construction of the Thermal Conductivity Cell. The thermal conductivity of aqueous $Sr(NO_3)_2$ and $LiNO_3$ solutions was measured by a concentric-cylinders (steady) technique. The apparatus details were described in our previous publications.[1−3] The apparatus is schematically shown in Figure 1. The main part of the apparatus consisted of a high-pressure autoclave, thermostat, and thermal conductivity cell. The thermal conductivity cell is schematically shown in Figure 2. The thermal conductivity cell consisted of two coaxial cylinders: inner

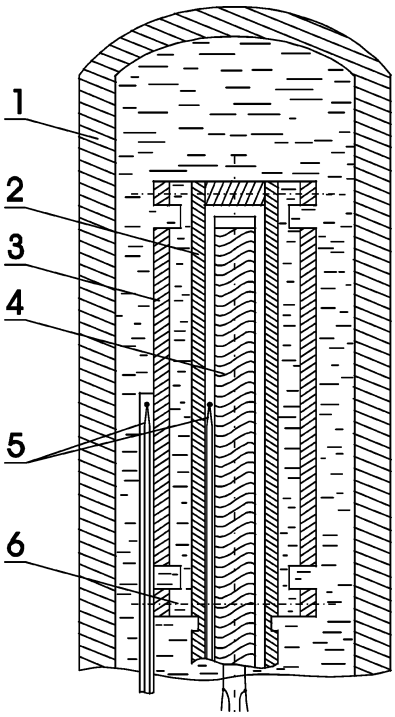

Figure 2. Schematic diagram of the measuring thermal conductivity cell. 1, Autoclave; 2, inner cylinder; 3, outer-cylinder; 4, microheater; 5, thermocouples; 6, axial alignment screws.

(emitting) cylinder (2) and outer (receiving) cylinder (3). The cylinders were made from stainless steel (1 × 18H9T, 1chrome-18nickel-9titanium, US designation S31600) and located in high-pressure autoclave (1). The support of the cylinders was provided by the porcelain rings with three centering microscrews (6), which were made from ceramic. The centering of the outer and inner cylinders was achieved by a microscrew. The deviation from concentricity was 0.002 cm or 2% of the sample layer. The quality of the centering was checked with a cathetometer (KM-8). To minimize of the conicity of cylinders, the surfaces of the inner and outer cylinders were perfectly polished with powder of a successively smaller grain size (320 nm). The cylindricality of the outer cylinder was checked with a microscope (YIM-21). In the lower part, inner cylinder extension was soldered by a flange. A flange was used to seal the autoclave. To this flange was also soldered a shell capillary, tightly fitted to the outer cylinder.

The autoclave was made from stainless steel 1X18H10T and located in the thermostat (2). The thermostat was a solid (massive) copper block. Temperature in the thermostat was controlled by the heater (3). The thermostat is supplied with three sectioned heating elements, a platinum resistant thermometer (PRT, 10) and three chromel−alumel thermocouples that were located on three different levels of the copper block. The temperature differences between various sections (levels) of the copper block were within 0.02 K. Temperature was measured with a PRT and with three chromel−alumel thermocouples (5). Thermocouples were located on different levels of the thermostat to minimize the inhomogeneities of temperature. One of the junctions of the differential chromel−copel thermocouple was located in the inner cylinder and tightly applied to the cylinder's wall. The second junction of the thermocouple was located in the shell capillary. Thermocouples were twice calibrated with a standard resistance thermometer. The difference between calibrations was 10 mK. The temperature-sensitive element of the thermocouple was located on the same level as measured cell. The reading of the single thermocouples differs by ±10 mK. The measurements were started when differences of readings of all the thermocouples were minimal (0.02 K).

Geometrical Characteristics of the Thermal Conductivity Cell. The important dimensions of the thermal conductivity cell are: o.d. of the inner cylinder is $d_2 = (10.98 \pm 0.01) \times 10^{-3}$ m. i.d. of the outer cylinder is $d_1 = (12.92 \pm 0.02) \times 10^{-3}$ m. The length of the measuring section of the inner cylinder (emitter) is $l = (150 \pm 0.1) \times 10^{-3}$ m. The gap between cylinders (thickness of the liquid gap) was $d = (0.97 \pm 0.03) \times 10^{-3}$ m. The choice of this gap was a compromise between decreasing convection and accommodation effect. The acceptable value for the thickness of the liquid layer d is between 0.5 and 1 mm. If $d > 1$ mm, the natural convection heat transfer will develop. The optimal value ratio of the length l to the diameter of the inner cylinder d_2 should be $l/d_2 = 10-15$. It is very difficult to keep the homogeneity of the temperature distribution along the length of inner cylinder when the ratio $l/d_2 > 15$. If $l/d_2 < 10$, the influence of the end effect is significant.

The solution under investigation is confined in the vertical gap of the cell. The thermal conductivity cell was filled with a sample using the set of valves (7, see Figure 1). Before filling, the cell was heated and evacuated. To fill the measuring cell (gap between cylinders) with a test liquid sample, the slots in a width of 2 mm and 25 mm in length were made on the outer cylinder (3 mm from the end). Pressure in the system was created and measured with piston manometers MP-600 and MP-60 with upper limit measurements of 600 and 60 bar, respectively. Mercury in the U-shape capillary tube was used as the separating liquid between oil and the sample. All connecting tubes, including filling unit and high-pressure U-shape separated vessels, were made from stainless steel.

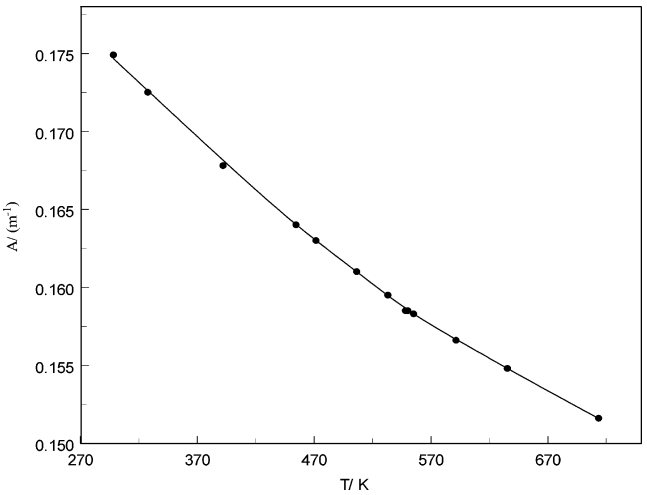

Figure 3. Geometrical constant A as a function of temperature from calibration with water. ●, experimental values of A. The solid curve is a guide to the eye.

In the cell, heat was generated in the microheater (4, see Figure 2) which consists of an isolated (high-temperature lacquer-covered) constantan wire of 0.1 mm diameter. A microheater was mounted inside the inner cylinder (emitter), which was close wound around a surface of a 2 mm diameter ceramic tube and isolated with high-temperature lacquer. The tube is tightly fitted in the heater pocket with a diameter of 6 mm on the inner cylinder. All heaters were made with 0.1 mm diameter constantan wire and isolated with high-temperature lacquer.

The electrical schema of the measurements consists of circuits of PRT, calorimetric heater, and differential and single thermocouples. All electrical measurements were performed with the compensation method using direct-current semiautomatic potentiometers (P323/2).

Principles of Operation, Working Equation, and Corrections. With this method, the heat generated in an inner emitting cylinder is conducted radially through the narrow fluid-filled annulus to a coaxial receiving cylinder. In this method, the thermal conductivity λ of the fluid was deduced from measurements of heat Q transmitted across the solution layer, the temperature difference ΔT between the inner and outer cylinders, the thickness of the solution layer d, and effective length l of measuring part of the cylinder (effective length of the cylinders).

The thermal conductivity of the sample at a given temperature and pressure was calculated from the relation

$$\lambda = \frac{Q \ln(d_2/d_1)}{2\pi l \Delta T} \qquad (2)$$

where $Q = Q_{meas} - Q_{los}$ is the amount of heat transferred by conduction alone across the sample layer between the cylinders, Q_{meas} is the amount of heat released by the calorimetric microheater, Q_{los} is the amount of heat losses through the ends of the measuring cell (end effect), d_1 is the outer diameter of the inner cylinder, d_2 is the inner

Table 1. Comparison between Experimental Thermal Conductivity Data and Values Calculated with IAPWS[16] Standard for Pure Water (AAD = 0.44%)

	P/MPa = 0.1		P/MPa = 10		P/MPa = 30		P/MPa = 60	
T/K	this work	λ/W·m^{-1}·K^{-1} IAPWS[16]	this work	λ/W·m^{-1}·K^{-1} IAPWS[16]	this work	λ/W·m^{-1}·K^{-1} IAPWS[16]	this work	λ/W·m^{-1}·K^{-1} IAPWS[16]
308.4	0.621	0.624	0.630	0.628	0.640	0.637	0.655	0.651
329.2	0.648	0.650	0.655	0.655	0.660	0.664	0.675	0.678
366.5	0.671	0.677	0.681	0.682	0.686	0.693	0.706	0.708
383.3			0.685	0.687	0.695	0.698	0.713	0.715
408.3			0.689	0.690	0.702	0.702	0.719	0.720
439.5			0.686	0.685	0.695	0.699	0.717	0.719
464.5			0.678	0.675	0.694	0.691	0.710	0.714
507.9			0.645	0.645	0.672	0.665	0.695	0.693
529.7			0.625	0.621	0.642	0.645	0.680	0.676
554.7			0.587	0.585	0.620	0.616	0.658	0.652
602.3					0.542	0.538	0.590	0.592
627.3					0.490	0.487	0.557	0.553
704.2					0.158	0.162	0.415	0.416

Table 2. Comparison between Experimental Thermal Conductivity Data and Values Calculated with Prediction Correlation (Lemmon et al.,[23] REFPRO) for Toluene (AAD = 2.2%)

	P/MPa = 0.1		P/MPa = 10		P/MPa = 30		P/MPa = 60	
T/K	this work	λ/W·m^{-1}·K^{-1} Lemmon et al.[23]	this work	λ/W·m^{-1}·K^{-1} Lemmon et al.[23]	this work	λ/W·m^{-1}·K^{-1} Lemmon et al.[23]	this work	λ/W·m^{-1}·K^{-1} Lemmon et al.[23]
300.6	0.131	0.130	0.135	0.133	0.140	0.139	0.152	0.147
334.7	0.125	0.119	0.122	0.123	0.134	0.130	0.150	0.143
359.4	0.117	0.113	0.116	0.117	0.129	0.124	0.141	0.138
376.4	0.114	0.109	0.115	0.113	0.126	0.121	0.135	0.130
430.7			0.106	0.102	0.116	0.111	0.124	0.121
494.5			0.092	0.091	0.105	0.102	0.114	0.113
549.6			0.082	0.082	0.097	0.096	0.108	0.108
593.7			0.080	0.077	0.094	0.092	0.106	0.105
668.8			0.078	0.070	0.093	0.088	0.104	0.102

Table 3. Test Measurements of the Thermal Conductivity of H_2O + NaCl Solution along the Isobar 20 MPa and Composition of 4.278 mol·kg^{-1}

	λ/W·m^{-1}·K^{-1}				
T/ K	this work	Abdulagatov and Magomedov[5]	El'darov[25]	Nikolaev[26]	Nagasaka et al.[27]
293.15	0.582	0.580	0.590	0.578	0.580
333.15	0.636	0.635	0.639	0.629	0.630
373.15	0.667	0.665	0.666	0.656	-
423.15	0.673	0.672	0.674	0.658	-
473.15	0.652	0.647	0.667	0.636	-
523.15	0.597	-	-	0.585	-
573.15	0.516	-	-	0.506	-
AAD	-	0.34%	0.88%	1.72%	0.64%

diameter of the outer cylinder, l is the length of measuring part of the cylinder, ΔT is the temperature difference between inner and outer cylinders (across the sample layer). The values of Q and ΔT are measured indirectly, and some corrections are necessary. The temperature difference in the sample layer can be determined as

$$\Delta T = \Delta T_{meas} - \Delta T_{corr} \tag{3}$$

where $\Delta T_{corr} = \Delta T_{cl} + \Delta T_{lac}$, ΔT_{cl} and ΔT_{lac} are the temperature differences in the cylinder walls and lacquer coat, respectively, ΔT_{meas} is the temperature difference measured with differential thermocouples. It is difficult to estimate the values of the Q_{los} and ΔT_{corr} by calculation. In this work, the values of Q_{los} and ΔT_{corr} were estimated by measuring the standard liquids (water) with well-known thermal conductivity (IAPWS[16] standard). Calibration was made with pure water at 10 selected temperatures between (293.15 and 713.15) K and at 3 selected pressures between (0.1 and 60) MPa. The amount of heat flow Q and the temperature difference ΔT were 13.06 W and 3.5 K, respectively. The estimated value of Q_{los} is about 0.05 W. This value is negligible (0.38%) by comparison with the heat transfer by conduction Q = 13.06 W.

After all corrections were taken into account, the final working equation for the thermal conductivity can be written as

$$\lambda = A\frac{Q_{meas} - Q_{los}}{\Delta T_{meas} - \Delta T_{corr}} \tag{4}$$

where $A = \ln(d_2/d_1)/2\pi l$ is the geometric constant which can be determined with geometrical characteristics of the experimental cell. The values of A can be also determined by means of a calibration technique using thermal conductivity data for the reference fluid (pure water, IAPWS[16]). The values of the cell constant determined with both with geometrical characteristics of the experimental cell and by calibration techniques (pure water at temperature 293.15 K) are 0.1727 m^{-1} and 0.1752 m^{-1}, respectively. In this work, we used the value of A as a function of temperature derived using calibration procedure with pure water (IAPWS[16]). The variation of the geometrical constant A with temperature is shown in Figure 3. The geometrical constant A changes by 12% over the temperature range from (293.15 to 750.15) K. The change in the cell size due to pressure was considered negligible due to the low volume compressibility of stainless steel (1X18H9T).

Because of the large emitter size and the small fluid volume surrounding the emitter, no effect of accommodation was to be expected. The calibration of the cell was made at a pressure of 60 MPa to avoid corrections due to accommodation effect.

Convection Heat Transfer. Convection heat transfer increases with increasing values of the Rayleigh number (Ra). The thermal conductivity measurements between coaxial cylinders show that the convection regime is related to Ra (product of the Grashof−Prandtl numbers)

$$\mathrm{Ra} = \mathrm{GrPr} = \frac{g\alpha_p \Delta T d^3 C_p \rho^2}{\lambda \eta} \tag{5}$$

where Gr and Pr are the Grashof and Prandtl numbers,

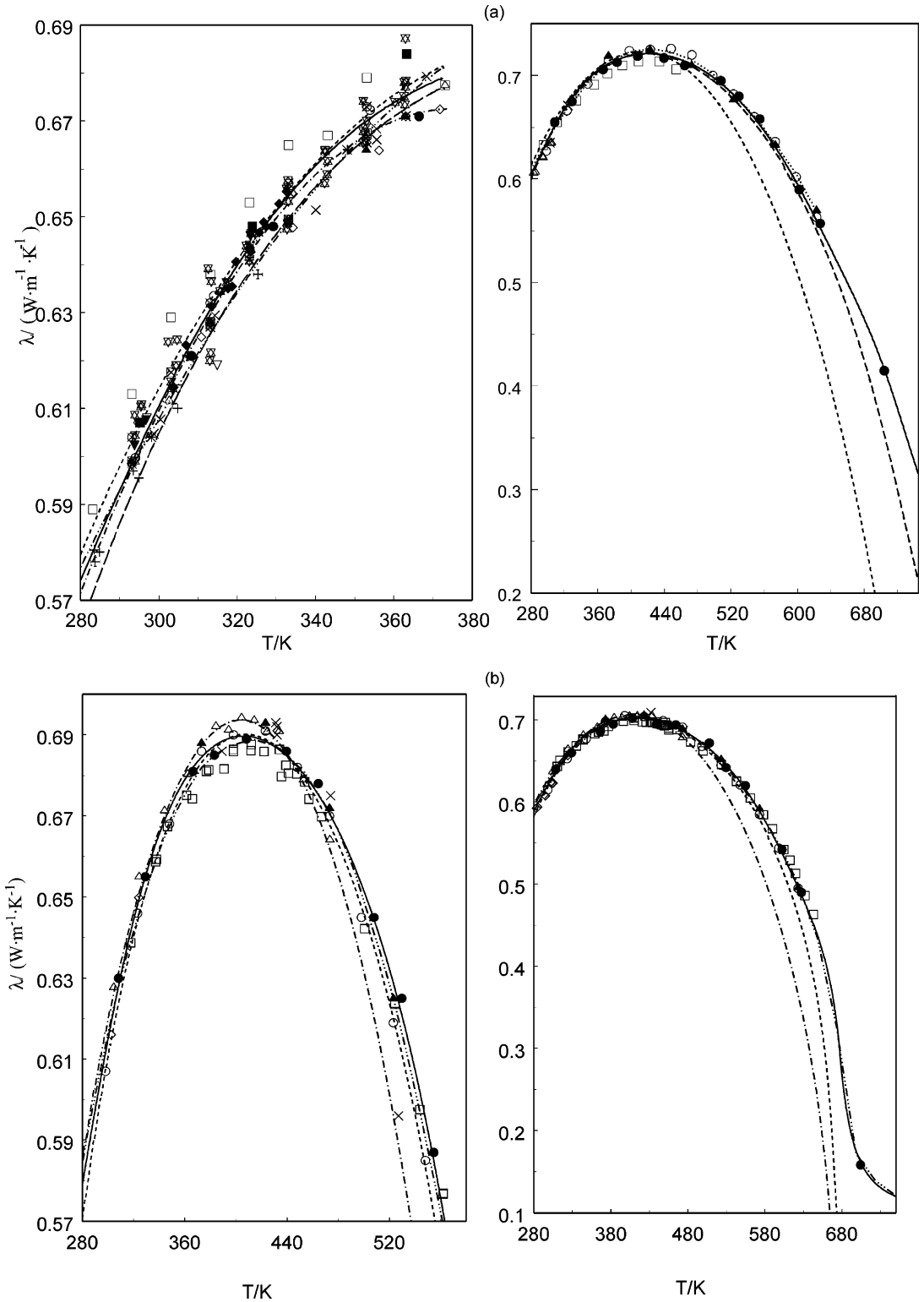

Figure 4. Measured values of thermal conductivity of pure H_2O as a function of temperature along the four isobars (0.1, 10, 30, and 60) MPa together with data and correlations reported by other authors in the literature. (a) $P = 0.1$ MPa: ●, this work; □, Takizawa et al.;[29] ×, Venart and Prasad;[30] ▽, Alloush et al.;[31] △, Ramires et al.;[21] ○, Nagasaka et al.;[27] ■, Rastorguev et al.;[32] ◇, Grigor'ev;[33] ▼, DiGuilio et al.;[34] ▲, Guseinov;[35] +, Castelli and Stanley;[36] ♦, Assael et al.;[37] ∗, Abdulagatov and Magomedov;[13] English cross, Davis et al.;[57] box with × inside, Vargaftik and Os'minin;[39] ✡, Lawson et al.;[40] box with vectorial product inside, Gazdiev and Rastorguev;[41] ⊹, Challoner and Powell;[42] ◻, Bach and Grigull;[43] ♂, Dix et al.;[44] Stupak et al.;[45] ◊, Tufeu et al.[46] —, calculated from the IAPWS[16] formulation; - · - · - ·-, Ramires et al.;[21] - - - -, Yata et al.;[47] - ··· - ··· - ··· -, Ripoche and Rolin;[48] – – – –, Dietz et al.[49] $P = 60$ MPa: ●, this work; —, calculated from the IAPWS[16] formulation; ○, Abdulagatov and Magomedov;[13] □, Grigor'ev;[33] ×, Dix et al.;[44] - - - -, Yata et al.;[47] ▲, Cherneyeva;[50] △, Castelli and Stanley;[36] – – – –, Dietz et al.;[49] ·····, Vargaftik et al.[51] (b) ●, this work; ○, Abdulagatov and Magomedov;[13] □, Le Neindre et al.;[52] △, Yata et al.;[47] ▲, Cherneyeva;[50] ◊, Dix et al.;[44] —, calculated from the IAPWS[16] formulation; - · - · - · -, Yata et al.;[47] - - - -, Dietz et al.[49]; - ··· - ··· - ··· -, Vargaftik et al.;[51] ×, Venart.[53]

respectively, g is the gravitational constant, α_p is the thermal expansion coefficient of the fluid, ρ is the density, C_P is the specific heat at constant pressure, η is the viscosity coefficient. To reduce the values of Ra, a small

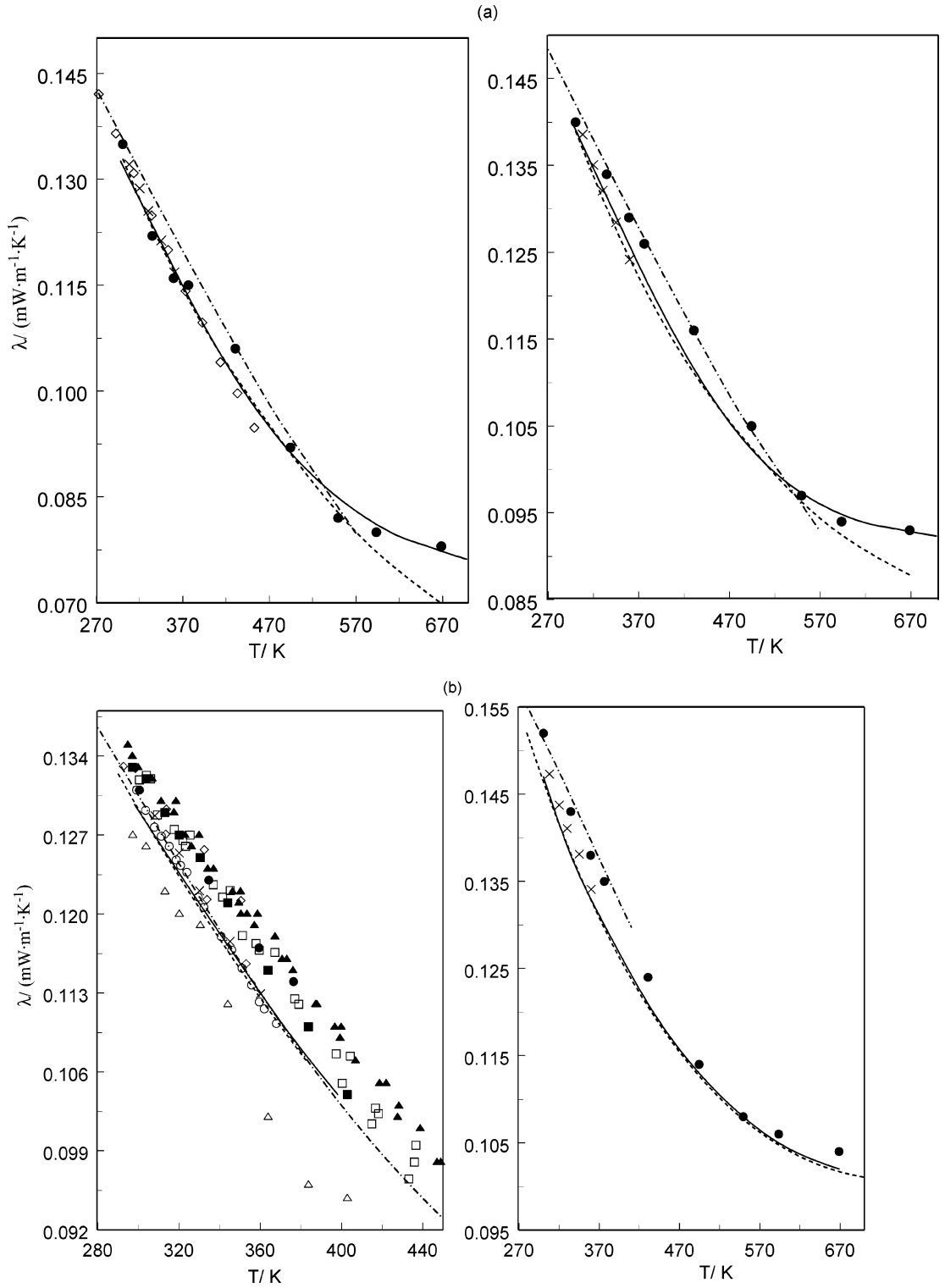

Figure 5. Measured values of thermal conductivity of toluene as a function of temperature along the four isobars, (0.1, 10, 30, and 60) MPa, together with values reported by other authors in the literature and calculated with various correlation and prediction equations. ●, this work; ○, Ramires et al.;[54] □, Geller et al.;[55] ▲, Rastorguev et al.;[56] △, Davis et al.;[57] ■, Ziebland;[38] ◊, Stupak et al.;[45] ×, Nieto de Castro et al.;[20] +, Yamada et al.;[58] solid line, Mamedov and Akhundov;[24] dashed line, Lemmon et al.[23] (REFPRO); dot-dashed line, Vargaftik et al.;[51] dotted line, Nieto de Castro et al.[20]

gap distance between cylinders $d = (0.97 \pm 0.03) \times 10^{-3}$ m was used. This makes it possible to minimize the risk of convection. Convection could develop when the Ra exceeds a certain critical value Ra_c, which for vertical coaxial cylinders is about 1000 (Gershuni).[17] Therefore, Ra > 1000 was considered as a criterion for the beginning of convection. In the range of the present experiments, the values of Ra were always less than 500 and Q_{con} was estimated to be negligibly small. The absence of convection can be verified experimentally by measuring the thermal conductivity with different temperature differences ΔT across the measurement gap and different power Q transferred from the inner to the outer cylinder. The measured thermal conductivity was indeed independent of the applied tem-

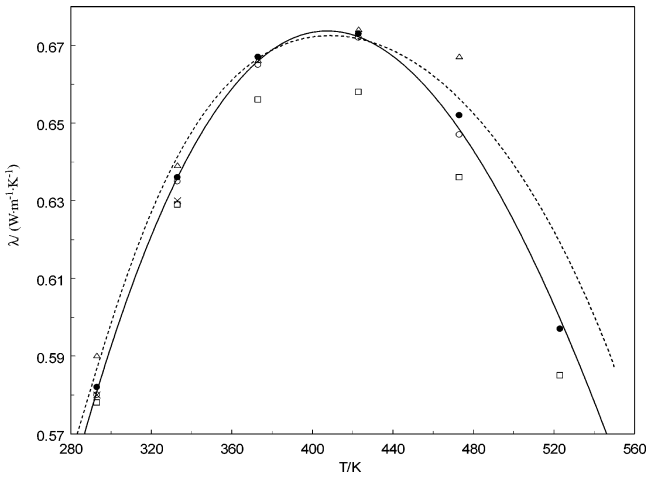

Figure 6. Measured values of thermal conductivity of H_2O + NaCl as a function of temperature along the isobar 20 MPa and concentration of 20 mass % together with values calculated with correlation equations and reported data from the literature. ●, this work; ○, Abdulagatov and Magomedov;[5] □, Nikolaev;[26] ×, Nagasaka et al.;[27] Δ, El'darov;[25] solid line, eq 1; dashed line, Chiquillo.[59]

perature differences ΔT and power Q transferred from inner to outer cylinder.

Heat Transfer by Radiation. Any conductive heat transfer must be accompanied by simultaneous radiative transfer. The correction depends on whether the fluid absorbs radiation. If the fluid is entirely transparent, then the conductive and radiative heat fluxes are additive and independent, and the simple correction given by Healy et al.[18] is adequate and usually negligible. When the fluid absorbs and re-emits radiation (partially transparent), the problem is more complicated since then the radiative and conductive fluxes are coupled. In this case, effect heat transferred by radiation can be derived from the solution integro-differential equation describing coupled radiation and conduction. This problem is amenable to exact study only numerically (Menashe and Wakeham,[19] Nieto de Castro et al.).[20] The approximate solution indicates that the magnitude of radiative contribution to the heat flux depends on the characteristic of the fluid for radiative absorption. This characteristic optical property of fluids is seldom known so that it is not possible to apply a correction for radiation routinely. There is some circumstance under which some contribution from radiative transport is negligible. The inner and outer cylinders were perfectly polished with powder of a successively smaller grain size (320 nm), their emissivity ($\epsilon = 0.32$) was small, and heat flux arising from radiation Q_{rad} is negligible by comparison with the heat transfer by conduction in the temperature range of our experiment. To minimize the heat transfer by radiation, the solid material (stainless steel 1 × 18H9T) of low emissivity was used for the cylinders and thin layers of fluid (from 0.97 mm) are used. In this way, heat transport by radiation can be strongly reduced compared to the heat transport by conduction. Because of the lack of characteristic optical properties of aqueous salt solutions at high temperatures, it is not possible to estimate theoretically the radiation conductivity λ_r and radiated heat Q_{rad}. The correction for absorption is small for pure water; therefore, for an aqueous solution in the temperature range up to 600 K and we assumed it negligible. Its influence on the uncertainty of the thermal conductivity is relatively small.

Since heat transfer by radiation is proportional to $4T^3\Delta T$, we would expect radiation losses to substantially increase with the cell temperature. In the present study, we did not study the influence of the cylinder wall emissivity on the conductive heat transfer. But this kind of correction is included in calibration procedure.

The values of the Q_{rad} can be estimated by calculation as

$$Q_{rad} = \epsilon\sigma S 4T^3\Delta T \qquad (6)$$

where $\epsilon = 0.32$ is the cylinder material emissivity coefficient, $\sigma = 5.67 \times 10^{-8}$ W·m^{-2}·K^{-4} is the Stefan−Boltzmann constant, and $S = 5.17 \times 10^{-3}$ m^2 is the mean surface of the fluid layer. The emissivity of walls was small and Q_{rad} (estimated by eq 6) is negligible (∼0.164 W) by comparison with the heat transfer (13.06 W) by conduction in the temperature range of our experiment.

Assessment of Uncertainties. Measurement uncertainties were associated with uncertainties that exist in measured quantities contained in working eq 4 used to compute the thermal conductivity from experimental data. The thermal conductivity was obtained from the measured quantities A, Q, T, ΔT, P, and m. The accuracy of the

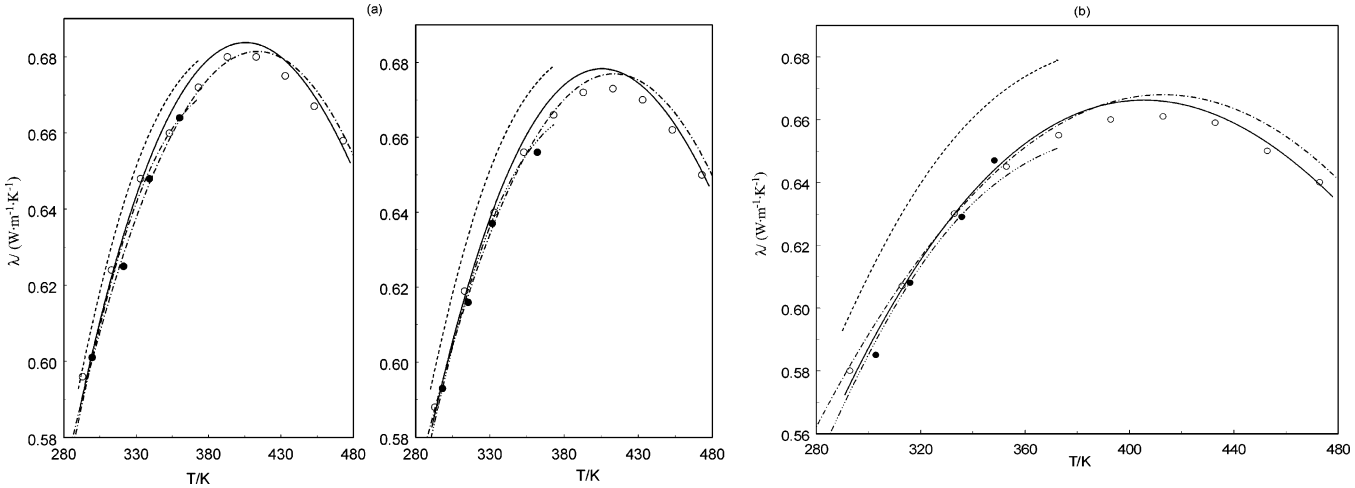

Figure 7. Measured values of thermal conductivity of H_2O + $Sr(NO_3)_2$ solutions as a function of temperature at atmospheric pressure for the three compositions (5, 10, 20 mass %) together with values calculated from various correlations and the data reported in the literature. ●, this work; ○, Abdulagatov and Magomedov;[4] solid line, calculated from eq 1; dot-dot-dot-dashed line, eq 9; dot-dashed line, Riedel;[60] dashed line, calculated from the IAPWS[16] formulation for pure water.

Table 4. Experimental Thermal Conductivities, Pressures, Temperatures, and Concentrations of H_2O + $Sr(NO_3)_2$ Solutions

	P/MPa = 10		P/MPa = 20		P/MPa = 30		P/MPa = 40	
m	T	λ	T	λ	T	λ	T	λ
mol·kg^{-1}	K	W·m^{-1}·K^{-1}	K	W·m^{-1}·K^{-1}	K	W·m^{-1}·K^{-1}	K	W·m^{-1}·K^{-1}
0.249	297.78	0.603	295.86	0.607	295.94	0.613	295.77	0.619
0.249	312.51	0.623	312.33	0.628	312.55	0.634	313.44	0.639
0.249	343.03	0.655	341.74	0.658	341.92	0.663	342.05	0.667
0.249	355.51	0.662	352.66	0.667	352.74	0.671	352.45	0.675
0.249	372.37	0.675	371.85	0.679	371.12	0.683	371.32	0.687
0.249	391.91	0.675	394.01	0.682	392.43	0.689	392.65	0.696
0.249	406.52	0.686	409.87	0.691	409.33	0.696	409.24	0.701
0.249	429.07	0.686	430.25	0.691	430.54	0.697	430.24	0.702
0.249	454.96	0.678	456.43	0.684	456.75	0.691	456.87	0.698
0.249	476.84	0.665	479.55	0.672	479.64	0.681	479.45	0.689
0.249	485.42	0.659	490.85	0.664	490.21	0.674	490.65	0.683
0.249	516.06	0.629	516.66	0.640	517.03	0.652	516.21	0.665
0.249	535.07	0.605	538.35	0.61	538.56	0.629	535.72	0.643
0.249	545.23	0.589	549.46	0.599	549.59	0.615	549.13	0.631
0.249	567.15	0.553	590.11	0.531	590.91	0.554	590.53	0.576
0.525	299.74	0.603	294.11	0.602	296.73	0.611	296.22	0.617
0.525	314.43	0.622	312.44	0.624	311.41	0.629	311.88	0.634
0.525	336.28	0.645	340.01	0.653	341.09	0.658	341.68	0.662
0.525	351.43	0.657	352.42	0.662	351.84	0.665	351.72	0.670
0.525	374.16	0.671	373.78	0.675	372.37	0.679	372.29	0.683
0.525	390.23	0.678	391.16	0.682	392.82	0.687	392.11	0.691
0.525	412.21	0.682	411.29	0.686	410.29	0.691	410.76	0.695
0.525	432.11	0.680	457.71	0.679	431.29	0.691	431.92	0.697
0.525	456.05	0.672	478.09	0.667	458.21	0.685	479.01	0.683
0.525	477.13	0.660	491.94	0.657	491.12	0.668	513.92	0.660
0.525	491.20	0.649	513.41	0.683	537.29	0.625	537.39	0.638
0.525	515.73	0.625	537.91	0.609	589.69	0.550	588.83	0.571
0.525	537.15	0.597	550.03	0.594				
0.525	553.82	0.573	590.34	0.527				
0.525	588.61	0.551						
1.181	299.64	0.597	299.41	0.602	298.44	0.607	298.01	0.612
1.181	314.72	0.615	314.79	0.620	318.72	0.629	318.22	0.633
1.181	336.72	0.636	336.52	0.641	337.82	0.646	337.15	0.650
1.181	351.88	0.649	351.25	0.653	350.28	0.656	350.92	0.660
1.181	374.12	0.663	374.07	0.667	377.69	0.671	377.89	0.675
1.181	390.68	0.669	390.02	0.672	391.52	0.677	390.83	0.680
1.181	412.73	0.672	412.47	0.676	415.63	0.681	415.19	0.685
1.181	432.73	0.671	432.73	0.675	433.30	0.680	433.54	0.685
1.181	456.26	0.663	456.94	0.669	455.41	0.675	455.93	0.681
1.181	477.21	0.650	477.80	0.658	475.08	0.667	475.67	0.674
1.181	491.32	0.640	491.35	0.648	492.18	0.656	492.57	0.664
1.181	515.87	0.616	515.03	0.626	514.70	0.638	515.06	0.648
1.181	537.58	0.588	536.89	0.601	536.42	0.615	536.99	0.628
1.181	553.52	0.565	553.74	0.579	552.42	0.595	552.39	0.610
1.181	588.02	0.503	589.33	0.522	589.22	0.540	588.64	0.560
2.025	297.73	0.588	296.04	0.592	298.75	0.600	298.03	0.605
2.025	317.58	0.611	314.72	0.612	316.55	0.619	316.84	0.623
2.025	338.41	0.629	340.09	0.636	339.15	0.639	339.88	0.643
2.025	351.48	0.641	353.77	0.646	352.16	0.648	352.75	0.652
2.025	375.38	0.656	377.50	0.658	376.77	0.661	377.02	0.665
2.025	394.36	0.661	417.73	0.664	395.75	0.668	395.03	0.671
2.025	412.26	0.663	436.79	0.665	410.74	0.670	410.94	0.674
2.025	437.42	0.660	455.95	0.659	434.60	0.669	434.20	0.674
2.025	458.74	0.652	476.20	0.648	456.29	0.664	455.89	0.669
2.025	477.12	0.641	492.15	0.637	475.84	0.655	475.09	0.662
2.025	489.29	0.630	516.32	0.610	491.41	0.645	490.95	0.652
2.025	519.77	0.601	535.06	0.594	520.02	0.621	519.92	0.631
2.025	537.88	0.581	551.34	0.573	535.32	0.604	534.93	0.616
2.025	554.51	0.558	590.11	0.510	552.83	0.584	552.06	0.598
2.025	568.27	0.534			591.17	0.527	591.06	0.545
3.150	297.55	0.581	297.53	0.586	298.76	0.598		
3.150	317.47	0.604	317.20	0.608	318.75	0.617		
3.150	338.19	0.623	338.46	0.626	337.05	0.632		
3.150	351.67	0.633	351.07	0.636	350.52	0.642		
3.150	375.93	0.645	375.21	0.648	377.66	0.655		
3.150	394.73	0.651	394.05	0.654	391.88	0.659		
3.150	412.49	0.653	412.89	0.656	415.25	0.663		
3.150	437.90	0.650	437.83	0.654	433.74	0.662		
3.150	458.93	0.642	458.27	0.647	455.19	0.658		
3.150	477.28	0.631	477.49	0.637	475.18	0.650		
3.150	489.43	0.622	489.62	0.629	492.29	0.640		
3.150	519.82	0.593	519.55	0.602	514.30	0.624		
3.150	537.13	0.571	537.32	0.581	536.87	0.604		
3.150	554.07	0.547	554.79	0.559	552.79	0.586		
3.150	585.77	0.494	585.09	0.511	589.54	0.537		

Table 5. Experimental Thermal Conductivity, Temperatures, and Compositions of H_2O+$Sr(NO_3)_2$ Solutions at Atmosperic Pressure

	P/MPa = 0.1			P/MPa = 0.1			P/MPa = 0.1			P/MPa = 0.1	
m/mol·kg^{-1}	T/K	λ/W·m^{-1}·K^{-1}	m/mol·kg^{-1}	T/K	λ/W·m^{-1}·K^{-1}	m/mol·kg^{-1}	T/K	λ/W·m^{-1}·K^{-1}	m/mol·kg^{-1}	T/K	λ/W·m^{-1}·K^{-1}
0.249	299.55	0.601	0.525	315.47	0.616	1.181	335.91	0.629	2.025	358.03	0.640
0.249	321.39	0.625	0.525	331.71	0.637	1.181	348.38	0.647	3.150	303.75	0.581
0.249	339.18	0.648	0.525	362.07	0.656	2.025	299.78	0.581	3.150	314.02	0.592
0.249	360.07	0.664	1.181	302.98	0.585	2.025	318.92	0.605	3.150	334.71	0.613
0.525	298.12	0.593	1.181	316.03	0.608	2.025	336.72	0.623	3.150	352.30	0.632

Table 6. Experimental Thermal Conductivities, Pressures, Temperatures, and Compositions of H_2O+ $LiNO_3$ Solutions

		λ/W·m^{-1}·K^{-1}					λ/W·m^{-1}·K^{-1}	
m/mol·kg^{-1}	T/K	P/MPa = 10	P/MPa = 20	P/MPa = 30	m/mol·kg^{-1}	T/K	P/MPa = 10	P/MPa = 20	P/MPa = 30
1.0	293.15	0.592	0.595	0.610	2.8	293.15	0.564	0.570	0.575
1.0	313.15	0.616	0.623	0.629	2.8	313.15	0.587	0.594	0.601
1.0	333.15	0.640	0.645	0.649	2.8	333.15	0.610	0.615	0.621
1.0	353.15	0.653	0.658	0.664	2.8	353.15	0.622	0.629	0.636
1.0	373.15	0.670	0.676	0.680	2.8	373.15	0.632	0.640	0.648
1.0	393.15	0.671	0.678	0.684	2.8	393.15	0.641	0.648	0.656
1.0	413.15	0.673	0.682	0.690	2.8	413.15	0.645	0.650	0.660
1.0	433.15	0.673	0.681	0.690	2.8	433.15	0.642	0.651	0.661
1.0	453.15	0.664	0.673	0.681	2.8	453.15	0.630	0.645	0.656
1.0	473.15	0.657	0.669	0.681	2.8	473.15	0.626	0.639	0.651
1.0	493.15	0.639	0.653	0.667	2.8	493.15	0.610	0.621	0.635
1.0	513.15	0.624	0.641	0.658	2.8	513.15	0.594	0.610	0.621
1.0	533.15	0.600	0.615	0.630	2.8	533.15	0.572	0.586	0.599
1.0	553.15	0.574	0.597	0.621	2.8	553.15	0.544	0.565	0.587
1.0	573.15	0.538	0.560	0.580	2.8	573.15	0.509	0.533	0.554
1.7	293.15	0.580	0.585	0.591	3.9	293.15	0.542	0.550	0.558
1.7	313.15	0.605	0.612	0.618	3.9	313.15	0.570	0.577	0.584
1.7	333.15	0.624	0.632	0.640	3.9	333.15	0.593	0.603	0.612
1.7	353.15	0.640	0.647	0.653	3.9	353.15	0.604	0.611	0.619
1.7	373.15	0.654	0.659	0.665	3.9	373.15	0.620	0.629	0.636
1.7	393.15	0.659	0.666	0.673	3.9	393.15	0.622	0.630	0.639
1.7	413.15	0.662	0.673	0.681	3.9	413.15	0.625	0.632	0.640
1.7	433.15	0.661	0.670	0.678	3.9	433.15	0.623	0.633	0.643
1.7	453.15	0.653	0.662	0.670	3.9	453.15	0.615	0.625	0.632
1.7	473.15	0.645	0.657	0.669	3.9	473.15	0.607	0.620	0.633
1.7	493.15	0.630	0.643	0.652	3.9	493.15	0.587	0.605	0.621
1.7	513.15	0.612	0.629	0.646	3.9	513.15	0.575	0.591	0.607
1.7	533.15	0.590	0.605	0.630	3.9	533.15	0.550	0.572	0.590
1.7	553.15	0.562	0.585	0.608	3.9	553.15	0.526	0.546	0.566
1.7	573.15	0.531	0.562	0.590	3.9	573.15	0.495	0.510	0.525

Table 7. Experimental Thermal Conductivity, Temperatures, and Concentrations of H_2O + $LiNO_3$ Solutions at P = 0.1 MPa

m/mol·kg^{-1}	T/K	λ/W·m^{-1}·K^{-1}	m/mol·kg^{-1}	T/K	λ/W·m^{-1}·K^{-1}	m/mol·kg^{-1}	T/K	λ/W·m^{-1}·K^{-1}
1.0	293.15	0.585	1.7	323.15	0.610	2.8	353.15	0.616
1.0	298.15	0.592	1.7	328.15	0.615	2.8	358.15	0.619
1.0	303.15	0.598	1.7	333.15	0.619	2.8	363.15	0.622
1.0	308.15	0.604	1.7	338.15	0.624	2.8	368.15	0.625
1.0	313.15	0.611	1.7	343.15	0.628	2.8	373.15	0.627
1.0	318.15	0.616	1.7	348.15	0.632	3.9	293.15	0.539
1.0	323.15	0.622	1.7	353.15	0.635	3.9	298.15	0.546
1.0	328.15	0.627	1.7	358.15	0.638	3.9	303.15	0.552
1.0	333.15	0.631	1.7	363.15	0.641	3.9	308.15	0.557
1.0	338.15	0.636	1.7	368.15	0.644	3.9	313.15	0.563
1.0	343.15	0.640	1.7	373.15	0.647	3.9	318.15	0.568
1.0	348.15	0.644	2.8	293.15	0.557	3.9	323.15	0.573
1.0	353.15	0.647	2.8	298.15	0.563	3.9	328.15	0.578
1.0	358.15	0.651	2.8	303.15	0.569	3.9	333.15	0.582
1.0	363.15	0.654	2.8	308.15	0.575	3.9	338.15	0.586
1.0	368.15	0.656	2.8	313.15	0.581	3.9	343.15	0.590
1.0	373.15	0.663	2.8	318.15	0.586	3.9	348.15	0.594
1.7	293.15	0.574	2.8	323.15	0.591	3.9	353.15	0.597
1.7	298.15	0.581	2.8	328.15	0.596	3.9	358.15	0.600
1.7	303.15	0.587	2.8	333.15	0.601	3.9	363.15	0.603
1.7	308.15	0.593	2.8	338.15	0.605	3.9	368.15	0.605
1.7	313.15	0.599	2.8	343.15	0.609	3.9	373.15	0.610
1.7	318.15	0.605	2.8	348.15	0.612			

thermal conductivity measurements was assessed by analyzing the sensitivity of eq 4 to the experimental uncertainties of the measured quantities. The maximum relative root-mean-square deviations ($\delta\lambda/\lambda$) of thermal conductivity

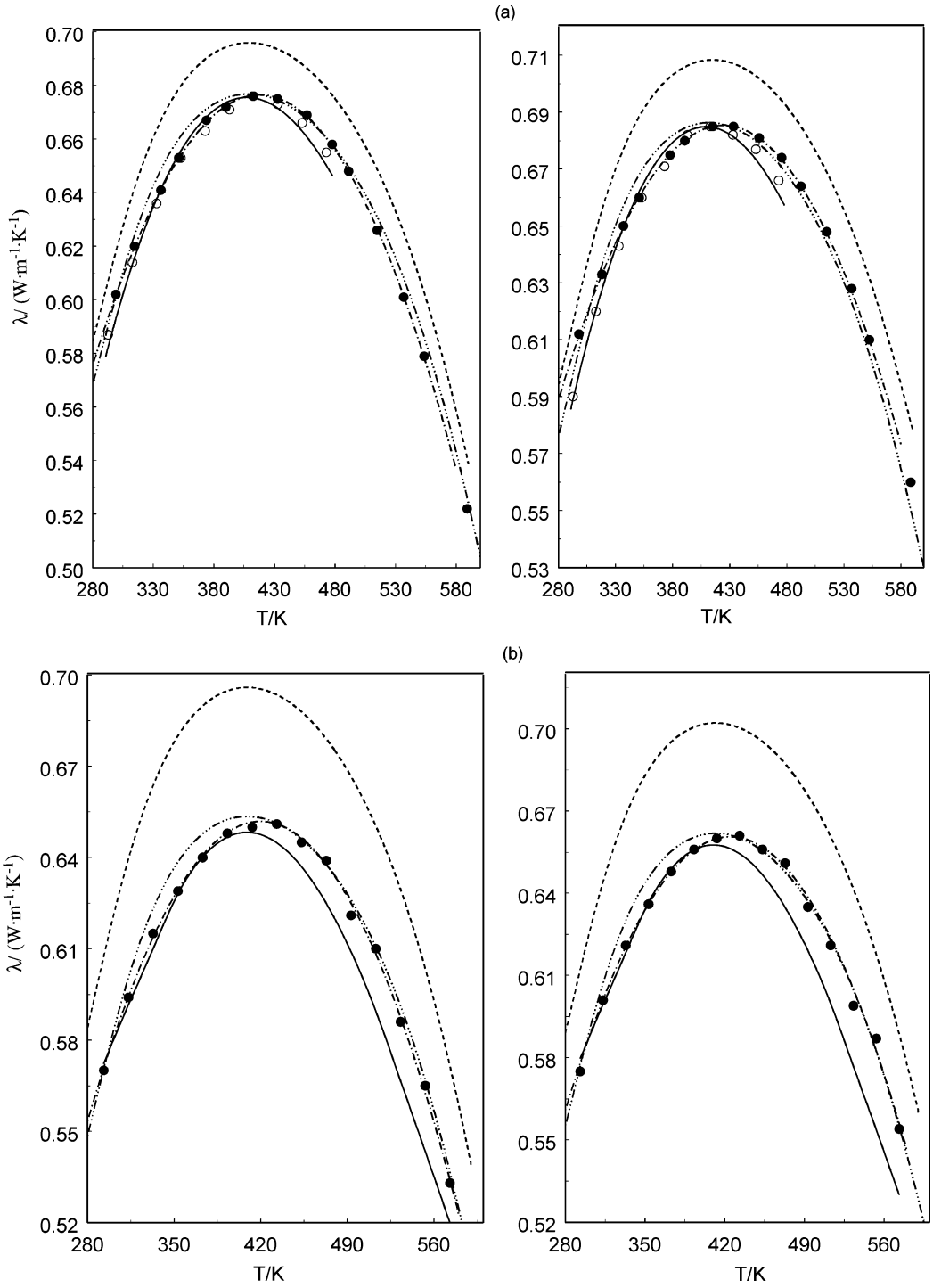

Figure 8. Measured values of thermal conductivity of H_2O + $Sr(NO_3)_2$ (a) and H_2O+ $LiNO_3$ (b) solutions as a function of temperature for various pressures and compositions together with values calculated from various correlations and the data reported in the literature. ●, this work; ○, Abdulagatov and Magomedov;[4] solid line, calculated from eq 1; dot-dashed line, eq 9; dot-dot-dot-dashed line, Riedel;[60] dashed line, calculated from the IAPWS[16] formulation for pure water.

measurements associated with A, Q, T, ΔT, P, and m measurements can be estimated from the equation

$$\frac{\delta\lambda}{\lambda} = \frac{1}{\lambda}\left(\left(\frac{\partial\lambda}{\partial A}S_A\right)^2 + \left(\frac{\partial\lambda}{\partial Q}S_Q\right)^2 + \left(\frac{\partial\lambda}{\partial\Delta T}S_{\Delta T}\right)^2 + \left(\frac{\partial\lambda}{\partial T}S_T\right)^2 + \left(\frac{\partial\lambda}{\partial P}S_p\right)^2 + \left(\frac{\partial\lambda}{\partial m}S_m\right)^2\right)^{1/2} \quad (7)$$

where $S_A = 0.0009$ m^{-1}, $S_Q = 2.6 \times 10^{-3}$ W, $S_{\Delta T} = 0.005$ K, $S_T = 0.03$ K, $S_p = 0.03$ MPa, and $S_m = 0.0006$ kg·mol^{-1} are the root-mean-square deviations of A, Q, ΔT, T, P, and m measurements, respectively.

The value of root-mean-square deviation of heat losses through the ends of the measuring cell is about $S_{Q\text{los}} = 0.001$ W. As the uncertainties of the measured values d_1, d_2, and l are 0.15%, 0.09%, and 0.07%, respectively, the corresponding uncertainty of A is 0.5%. The experimental uncertainty in the concentration is estimated to be 0.02%.

Values for the partial derivatives $(\partial\lambda/\partial P)_T$, $(\partial\lambda/\partial T)_P$, and $(\partial\lambda/\partial m)_{P,T}$ have been calculated using the correlating equation for thermal conductivity reported in the next section (see below eq 9) for various experimental path (isotherm−isopleth, isobar−isopleth, and isotherm−isobar). The maxi-

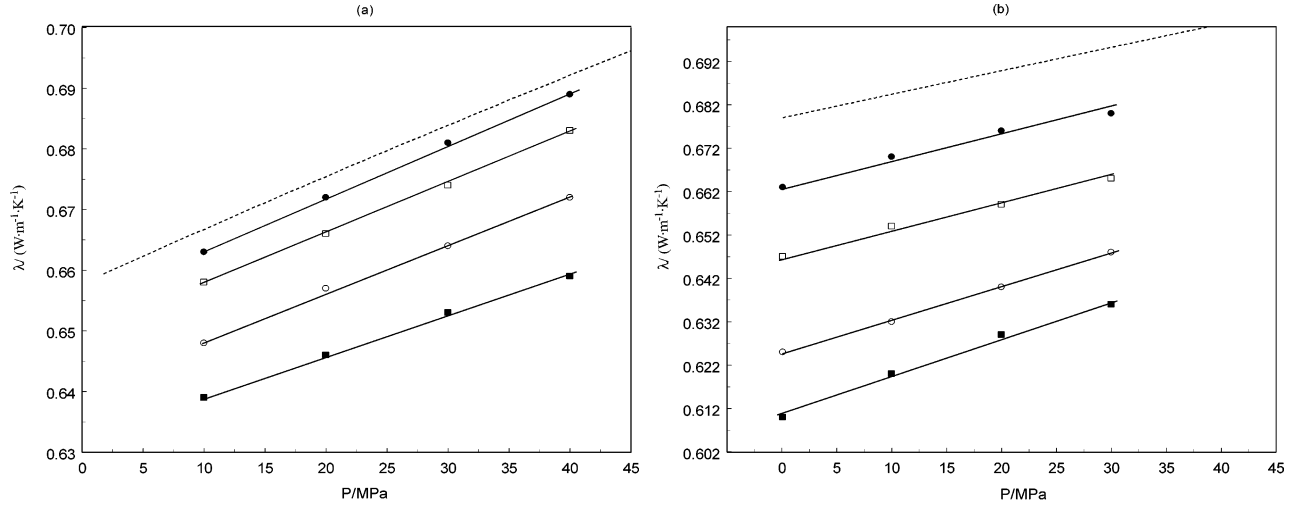

Figure 9. Measured values of thermal conductivity of $H_2O + Sr(NO_3)_2$ (a) and H_2O+ $LiNO_3$ (b) solutions as a function of pressure for various temperatures and compositions together with values of thermal conductivity for pure water calculated with the IAPWS[16] formulation. (a) $H_2O + Sr(NO_3)_2$, $T = 479.55$ K: ●, 0.249 mol·kg^{-1}; □, 0.525 mol·kg^{-1}; ○, 1.181 mol·kg^{-1}; ■, 2.015 mol·kg^{-1}. (b) H_2O + $LiNO_3$, $T = 373.15$ K: ●, 1.0 mol·kg^{-1}; □, 1.7 mol·kg^{-1}; ○, 2.8 mol·kg^{-1}; ■, 3.9 mol·kg^{-1}; solid line, calculated from eq 1; dashed line, calculated from the IAPWS[16] formulation for pure water.

Table 8. Deviation Statistics for $H_2O + Sr(NO_3)_2$ and H_2O + $LiNO_3$ Solutions

$H_2O+Sr(NO_3)_2$				
	m/mol·kg^{-1}			
deviation	0.249	0.525	1.181	2.025
AAD	1.00	0.87	0.72	0.95
bias	−0.10	0.20	0.44	0.95
std dev	1.14	0.90	0.82	0.56
std err	0.16	0.15	0.12	0.10
N	51	44	44	35
$H_2O+LiNO_3$				
	m/mol·kg^{-1}			
deviation	1.0	1.7	2.8	3.9
AAD	0.89	1.13	1.26	1.25
bias	−0.21	−0.63	−0.61	−0.60
std dev	1.03	1.16	1.25	1.37
std err	0.17	0.19	0.24	0.34
N	40	40	11	35

mum values of $(1/\lambda)(\partial\lambda/\partial P)_T$ and $(1/\lambda)(\partial\lambda/\partial T)_P$ were found to be 2×10^{-5} and 4×10^{-5}, respectively.

The systematic uncertainties of the thermal conductivity Θ_λ measurements can be estimated from the equation

$$\Theta_\lambda = \frac{1}{2}\left[\left(\frac{\partial^2\lambda}{\partial A^2}\right)S_A{}^2 + \left(\frac{\partial^2\lambda}{\partial Q^2}\right)S_Q{}^2 + \cdots + \left(\frac{\partial^2\lambda}{\partial P^2}\right)S_P{}^2\right] \quad (8)$$

The systematic uncertainties of the measured quantities are: $\theta_Q = 5.2 \times 10^{-4}$ W is the systematic uncertainty of the heat flow; $\theta_{\Delta T} = 0.001$ K is the systematic uncertainty of the temperature difference; $\theta_{Q\mathrm{los}} = 5.0 \times 10^{-4}$ W is the systematic uncertainty of the heat losses through the ends of the measuring cell. The uncertainty of temperature and pressure measurements are: $\theta_T = 0.02$ K and $\theta_P = 0.03$ MPa at pressures up to 60 MPa. The corresponding uncertainty of the thermal conductivity measurement related with uncertainties of temperature and pressure measurements is estimated to be less than 0.006%.

The uncertainty in heat flow Q measurement is about 0.1%. To make sure that the cell was in equilibrium, the measurements were started 10 hours after the time when the thermostat temperature reached the prescribed temperature. About 5−6 measurements are carried out at one state, and the average value of thermal conductivity is calculated. Reproducibility (scattering of the different measurements) of the measurements is about 0.5%.

From the uncertainty of the measured quantities and the corrections mentioned above, the total maximum relative uncertainty $\delta\lambda/\lambda$ in measuring the thermal conductivity was 2%. The relative systematic uncertainty Θ_λ/λ was 0.002. All of the other uncertainties were assumed negligible.

Performance Tests. To check and confirm the accuracy of the method and procedure of the measurements, thermal conductivity data were taken for pure water and toluene in the temperature range from (300.6 to 704.2) K at pressures up to 60 MPa and for aqueous NaCl solutions along the isobar of 20 MPa and concentration of 20 mass %. Tables 1 and 2 provide a detailed comparison present test measurement results for pure water and toluene with the reference data for water (IAPWS[16] and Ramires et al.[21]) and toluene (Ramires et al.,[22] Lemmon et al.,[23] and Mamedov and Akhundov[24]). The comparison between the present measurements for H_2O + NaCl solution with the data reported by other authors[5,25−27] is given in Table 3. Figures 4, 5 (parts a and b), and 6 also demonstrated the direct comparison between the present measurements of thermal conductivity for pure water, toluene, and H_2O + NaCl solution and the values calculated with various

Table 9. Parameters a_{ijk} of Equation 9

	$H_2O+Sr(NO_3)_2$				$H_2O+LiNO_3$			
	$i = 0$		$i = 1$		$i = 0$		$i = 1$	
k	$j = 0$	$j = 1$	$j = 0$	$j = 1$	$j = 0$	$j = 1$	$j = 0$	$j = 1$
0	0.5607×10^{0}	7.7556×10^{-4}	-4.8916×10^{-4}	-3.0969×10^{-6}	0.5697×10^{0}	9.0083×10^{-4}	-1.4940×10^{-2}	-4.3446×10^{-5}
1	1.7773×10^{-3}	-6.9969×10^{-6}	-5.0504×10^{-6}	5.8904×10^{-9}	-1.6694×10^{-3}	-9.2409×10^{-6}	-4.3451×10^{-5}	2.0500×10^{-6}
2	-6.3080×10^{-6}	3.7035×10^{-8}	1.5390×10^{-8}	-1.3926×10^{-10}	6.0137×10^{-6}	5.1106×10^{-8}	1.5168×10^{-7}	-8.3197×10^{-9}

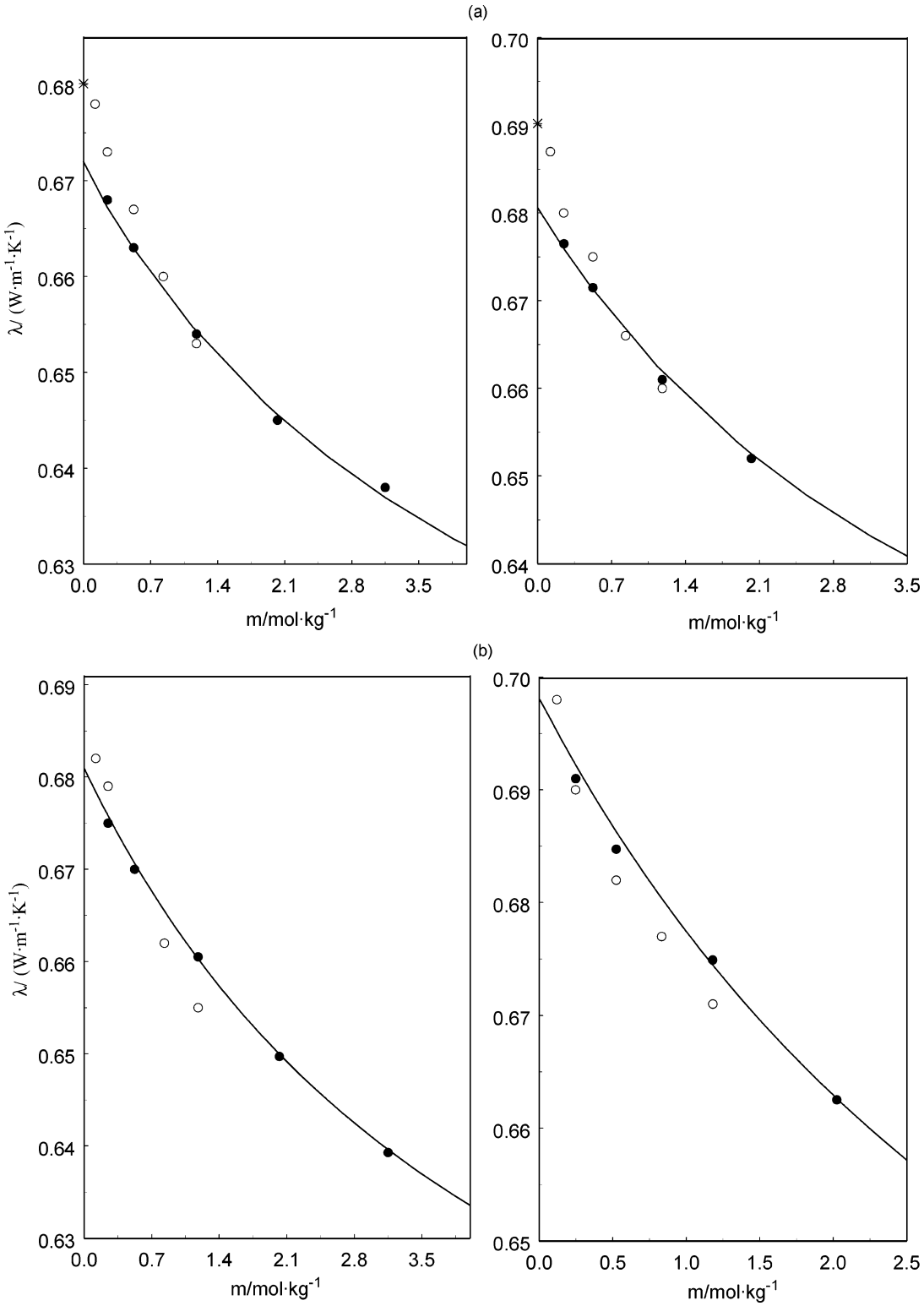

Figure 10. Comparison of the concentration dependence of the present thermal conductivity results for $H_2O + Sr(NO_3)_2$ solutions with the data reported in the literature at various temperatures and pressures. ●, this work; ○, Abdulagatov and Magomedov;[4] *, IAPWS[16] (pure water).

correlation equations and reported data from the literature. The NIST correlation by Lemmon et al.[23] (REFPRO) was developed without using any experimental data for toluene. This correlation was based on an extended corresponding-states model for the thermal conductivity developed by McLinden et al.[28] Therefore, the agreement between the present thermal conductivity measurements and prediction values of thermal conductivity for toluene (Lemmon et al.,[23] REFPRO) is acceptable (AAD = 2.2%, slightly exceeding the present experimental uncertainty). As Figure 4 (parts a and b) and Table 1 demonstrate, the agreement between test measurements for pure water and IAPWS[16] calculations is excellent (AAD = 0.44%, much lower than their experimental uncertainty). Excellent agreement is found between present thermal conductivity results for pure water and the data reported by other authors (AAD within 0.2 to 1.2%) and reference data reported by Ramires et al.[21] (AAD = 0.25%). The agreement between the literature

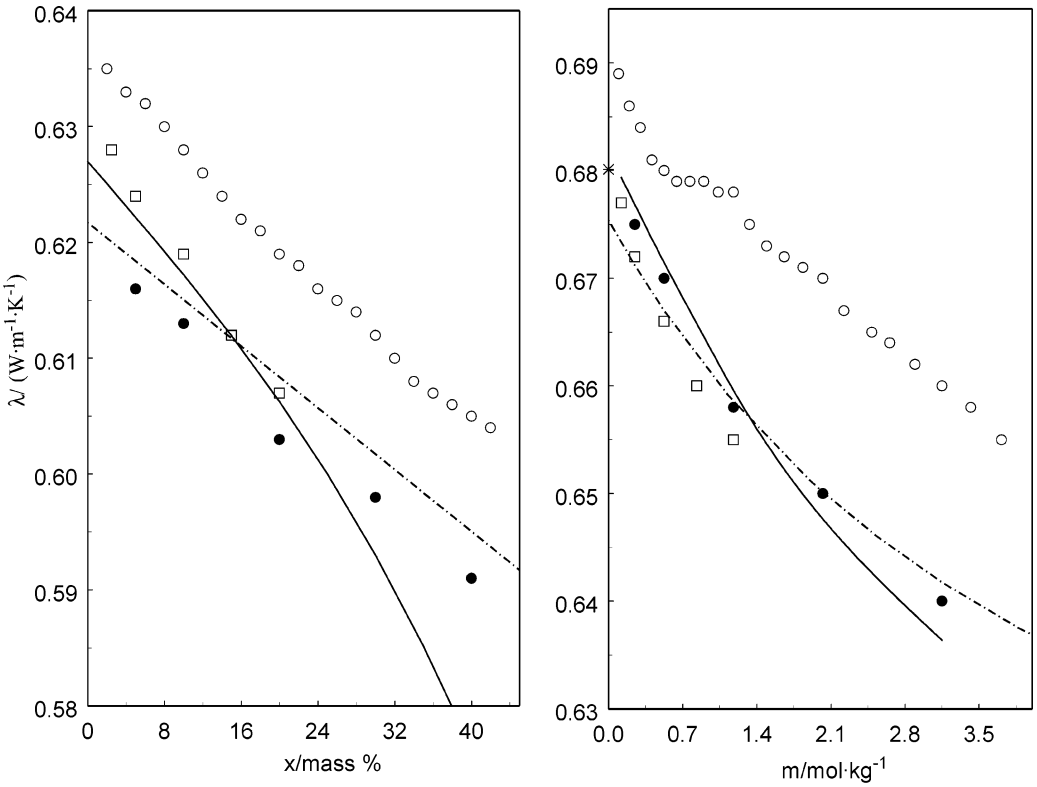

Figure 11. Measured values of thermal conductivity of $H_2O + Sr(NO_3)_2$ solutions as a function of concentration along two isotherms 353.15 K (a) and 473.15 (b) for pressures (20 and 40) MPa. ●, this work; □, Abdulagatov and Magomedov;[4] ○, Aseyev;[14] solid line, calculated from eq 1, dot-dashed line, eq 9.

data[5,25−27] for H_2O + NaCl solutions and the present measurements is within (0.34 to 1.72)% (see Table 3). This excellent agreement for test measurements confirms the reliability and accuracy of the present measurements for $H_2O + Sr(NO_3)_2$ and $H_2O + LiNO_3$ solutions and corrects operation of the instrument.

This thermal conductivity apparatus had been successfully employed in three previous studies of thermal conductivity of aqueous solutions[1−3] ($H_2O + Li_2SO_4$, $H_2O + Zn(NO_3)_2$, $H_2O + Ca(NO_3)_2$, and $H_2O + Mg(NO_3)_2$) at high temperatures and high pressures.

The solutions at the desired composition were prepared by mass. The composition was checked by comparison of the density of solution at 293.15 K and 0.1 MPa with reference data.

Results and Discussion

Measurements of the thermal conductivity for the aqueous $Sr(NO_3)_2$ solutions were performed along five isobars (0.1, 10, 20, 30, and 40) MPa between (294.11 and 591.06) K for five molalities, namely, (0.249, 0.525, 1.181, 2.025, and 3.150) mol·kg^{-1}, while for aqueous $LiNO_3$ solutions, measurements were made at four isobars (0.1, 10, 20, and 30) MPa for four molalities (1.0, 1.7, 2.8, and 3.9) mol·kg^{-1} between (293.15 and 573.15) K. The experimental temperature, pressure, composition, and thermal conductivity values are presented in Tables 4−7. The average temperature in the fluid layer equals $T_{aver} = T_1 + 0.5\Delta T$, where T_1 is the temperature of the outer cylinder and ΔT is the temperature difference across the measurement gap. The values of T_{aver} were accepted as experimental temperatures. Some selected experimental results are shown in Figures 7 (parts a and b) through 10 (parts a and b) as projections of isopleth−isotherm (constant composition and constant temperature), isobar−isotherm (constant pressure and constant temperature), and isopleth−isobar (constant composition and constant pressure) in the λ-T, λ-P, and λ-m spaces together with values calculated from IAPWS[16] for pure water and various correlation equations from the literature. The thermal conductivity of $H_2O + Sr(NO_3)_2$ and $H_2O + LiNO_3$ solutions was measured as a function of temperature at constant pressure for various compositions. In Figures 7 (parts a and b) and 8 (parts a and b), the temperature dependence of the measured values of thermal conductivity for the $H_2O + Sr(NO_3)_2$ and $H_2O + LiNO_3$ solutions along various isobars and compositions. On each isopleth−isobaric curve, the thermal conductivity shows its maximum value at temperatures between (406 and 437) K for $H_2O + Sr(NO_3)_2$ and between (413 and 433) K for $H_2O + LiNO_3$ depending of pressure and concentration. For pure water, this maximum occurs at temperatures between (409 and 421) K as pressure changing between (20 and 60) MPa. The thermal conductivity maximum is largely affected by composition and pressure. For example, for concentration of 0.525 mol·kg^{-1} at pressures of 10 MPa, the maximum in the thermal conductivity occurs at a temperature of about 415 K and shift to the high temperature of about 425 K as composition changes. At the same isobar (10 MPa), the maximum of thermal conductivity for pure water occurs at a temperature of 405 K. The pressure and composition dependence of the thermal conductivity maximum for aqueous salt solutions were studied by Abdulagatov and Magomedov.[9−12]

Figures 9 (parts a and b) shows the results of the thermal conductivity measurements for $H_2O + Sr(NO_3)_2$ and $H_2O + LiNO_3$ solutions as a function of pressure. Along each isopleth−isotherm, the thermal conductivity increases almost linearly as the pressure increase in the temperature range up to 591.06 K and at pressures up to 40 MPa. The composition dependences of the measured thermal conduc-

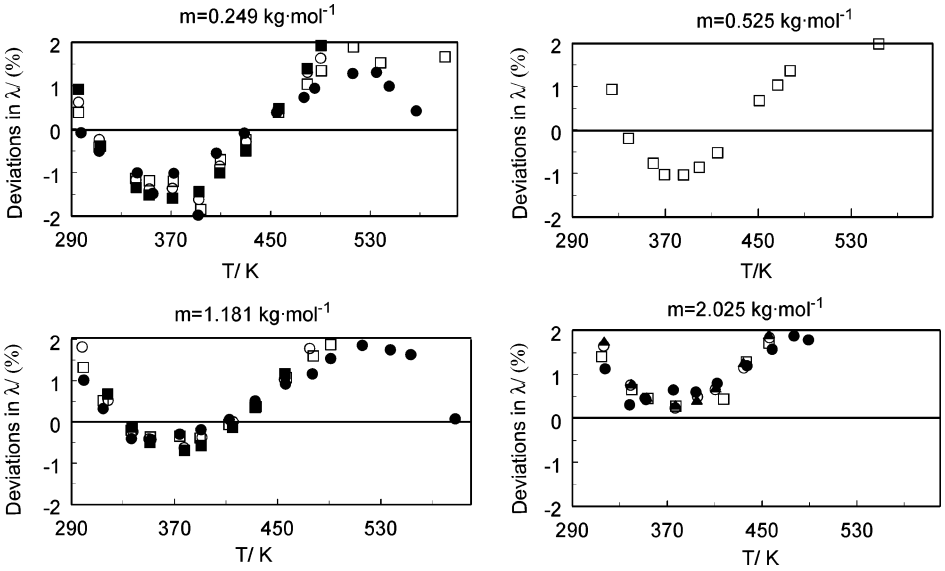

Figure 12. Percentage thermal conductivity deviations, $\delta\lambda = 100(\lambda_{exp} - \lambda_{cal})/\lambda_{cal}$, of the experimental thermal conductivities for H_2O + $Sr(NO_3)_2$ solutions from the values calculated with eq 1. ●, 10 MPa; □, 20 MPa; ○, 30 MPa; ■, 40 MPa.

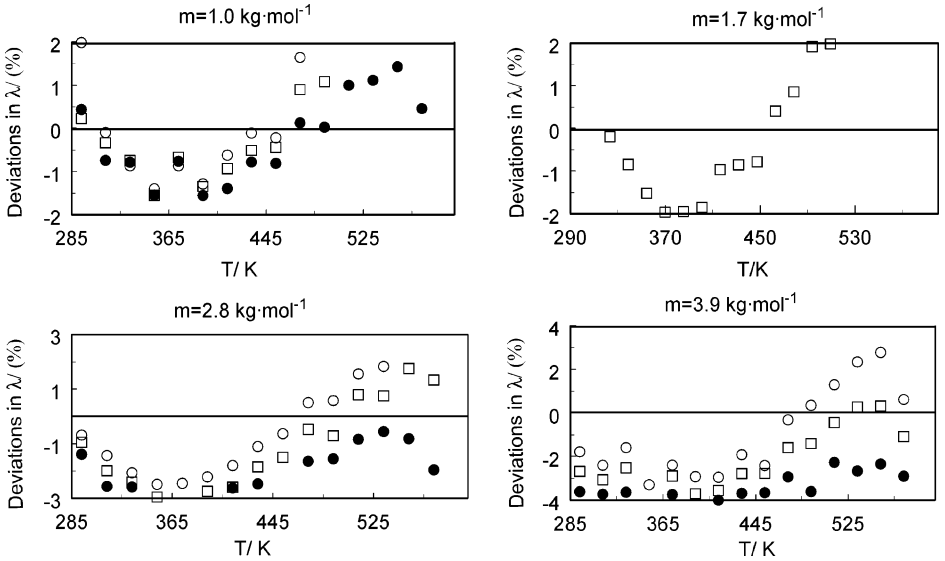

Figure 13. Percentage thermal conductivity deviations, $\delta\lambda = 100(\lambda_{exp} - \lambda_{cal})/\lambda_{cal}$, of the experimental thermal conductivities for H_2O + $LiNO_3$ solutions from the values calculated with eq 1. ●, 10 MPa; □, 20 MPa; ○, 30 MPa.

tivities for H_2O + $Sr(NO_3)_2$ solutions for two selected isotherms (353.15 and 473.15) K and two isobars (20 and 40) MPa are shown in Figure 10 (parts a and b), together with data reported by Abdulagatov and Magomedov.[4] The thermal conductivity of the solution monotonically decreases with composition. As one can see from Figure 10 (parts a and b), the composition dependence of the thermal conductivity exhibits a small curvature at high compositions (m > 1 mol·kg^{-1}). Extrapolation of the high composition measurements to zero concentration ($m \rightarrow 0$) gives values in good agreement with the data for pure water (see parts a and b of Figure 10). Figure 11 shows comparisons of the composition dependence of the present thermal conductivity data measurements for H_2O + $Sr(NO_3)_2$ solutions at atmospheric pressure for two isotherms (313.15 and 373.15) K with the data reported by Abdulagatov and Magomedov[4] and Aseyev.[14] As one can see from Figure 11, the data reported by Aseyev[14] is systematically higher (about 2.5%) than the present data and the data reported by Abdulagatov and Magomedov.[4] Figure 11 also illustrates the good consistency of the concentration dependence of thermal conductivity of H_2O + $Sr(NO_3)_2$ measured in present work and reported by Abdulagatov and Magomedov.[4]

The present results for thermal conductivity of H_2O + $Sr(NO_3)_2$ solutions at three pressures (0.1, 20, and 40) MPa can be directly compared with experimental values reported by Abdulagatov and Magomedov.[4] Figures 7 (parts a and b) and 8 (parts a and b) contain the values of thermal conductivity measured by Abdulagatov and Magomedov[4] and calculated from correlation eq 1 for H_2O + $Sr(NO_3)_2$ and H_2O + $LiNO_3$ solutions together with present results. The deviation plots are given in Figures 12 and 13. The deviation statistics of the comparisons between present thermal conductivity data and values calculated with correlation eq 1 for H_2O + $Sr(NO_3)_2$ and H_2O + $LiNO_3$ solutions are given in Table 8 for each measured composition. For all of the data, the AAD values are 0.89% and 1.1%, respectively, for H_2O + $Sr(NO_3)_2$ and H_2O + $LiNO_3$ solutions. Only extrapolation of the eq 1 to high temperatures (above 473.15 K) and to high compositions (above 25 mass %) describes the thermal conductivity of H_2O +

$Sr(NO_3)_2$ and $H_2O + LiNO_3$ solutions with an accuracy that exceeds their experimental uncertainty (2%). Figures 8 (parts a and b) illustrates that extrapolated values of thermal conductivity to validity out of range of the eq 1 are reasonably consistent with the present measurements. This is still good because the temperature, pressure, and concentration ranges where eq 1 is valid are (273.15 to 473.15) K, up to 100 MPa, and (0 to 25) mass %. Excellent agreement (within 0.5%) is fond between present data and values predicted by Riedel[60] equation.

Correlation

Because of the lack of theoretical background on the temperature, pressure, and composition, dependency of the thermal conductivity for aqueous salt solutions, empirical and semiempirical correlation equations, and prediction techniques are using the literature. The results of the (λ,P,T,m) measurements for $H_2O + Sr(NO_3)_2$ and $H_2O + LiNO_3$ solutions were represented by the equation

$$\lambda/\mathrm{W{\cdot}m^{-1}{\cdot}K^{-1}} = \sum_{i=0}^{1}\sum_{j=0}^{1}\sum_{k=0}^{2} a_{ijk} m^i P^j t^k \qquad (9)$$

where λ is the thermal conductivity of the solution, t is the temperature in °C, and P is the pressure in MPa.

At high concentrations ($m > 1$ mol·kg^{-1}), nonlinear terms for the composition dependence in eq 9 have to be included. Equation 9 describes the thermal conductivity of $H_2O + Sr(NO_3)_2$ and $H_2O + LiNO_3$ solutions with an accuracy that does not exceed their experimental uncertainty. The average absolute deviation between measured and calculated values with eq 9 is (0.5 to 0.7)%. The coefficients of eq 9 have been exclusively determined in order to minimize the mean quadratic deviation of the fitted experimental thermal conductivity values. The derived values of the coefficients a_{ij}, b_{ij}, c_{ij}, and d_{ij} in eq 9 for $H_2O + Sr(NO_3)_2$ and $H_2O + LiNO_3$ solutions are given in Table 9. Equation 9 is valid in the temperature range from (290.15 to 595.15) K, at pressures up to 40 MPa, and for composition up to 4 mol·kg^{-1}.

Conclusion

The thermal conductivities of five aqueous $Sr(NO_3)_2$ solutions (0.249, 0.525, 1.181, 2.025, and 3.150) mol·kg^{-1} and four aqueous $LiNO_3$ solutions (1.0, 1.7, 2.8, and 3.9) mol·kg^{-1} have been measured with a coaxial-cylinder (steady) technique. Measurements were made at five isobars (0.1, 10, 20, 30, and 40) MPa for $H_2O + Sr(NO_3)_2$ and at four isobars (0.1, 10, 20, and 30) MPa for $H_2O + LiNO_3$ solutions. The range of the temperature was (293.13 to 591.06) K. The total uncertainty of thermal conductivity, pressure, temperature, and composition measurements were estimated to be less than 2%, 0.05%, 30 mK, and 0.02%, respectively. The temperature, pressure, and concentration dependencies of thermal conductivity were studied. The measured values of thermal conductivity were compared with data and correlations reported in the literature. The reliability and accuracy of the experimental method was confirmed with measurements on pure water, toluene, and H_2O + NaCl. The experimental and calculated values of thermal conductivity for pure water from IAPWS[16] formulation show excellent agreement within their experimental uncertainties (AAD within 0.44%). Agreement between present test measurements for aqueous NaCl solution and the data sets reported in the literature is within (0.64 to 1.72) %. The correlation equation for thermal conductivity was obtained as a function of temperature, pressure, and composition by a least-squares method from the experimental data. The AAD between measured and calculated values of thermal conductivity for solutions from this correlation equation was 0.5−0.7%. The measured thermal conductivity values of solutions were compared with the data reported in the literature by other authors. Good agreement (deviations within 0.72 to 1.25%) is found between the present measurements and the data sets reported by other authors in the literature.

Acknowledgment

Abdulagatov I.M. thanks the Physical and Chemical Properties Division at the National Institute of Standards and Technology for the opportunity to work as a Guest Researcher at NIST during the course of this research.

Literature Cited

(1) Azizov, N. D. Thermal Conductivity of Aqueous Solutions of Li_2SO_4 and $Zn(NO_3)_2$. *Russ. High Temp.* **1999**, *37*, 649−651.
(2) Akhundov, T. C.; Iskenderov, A. I.; Akhmedova, L. A. Thermal Conductivity of Aqueous Solutions of $Ca(NO_3)_2$. *Izv. Vuzov, ser. Neft i Gas* **1994**, *3*, 49−52.
(3) Akhundov, T. C.; Iskenderov, A. I.; Akhmedova, L. A. Thermal Conductivity of Aqueous Solutions of $Mg(NO_3)_2$. *Izv. Vuzov, ser. Neft i Gas* **1995**, *1*, 56−58.
(4) Abdulagatov, I. M.; Magomedov, U. M. Thermal Conductivity Measurements of Aqueous $SrCl_2$ and $Sr(NO_3)_2$ Solutions in the Temperature Range Between 293 and 473 K at Pressures up to 100 MPa. *Int. J. Thermophys.* **1999**, *20*, 187−196.
(5) Abdulagatov, I. M.; Magomedov, U. B. Thermal Conductivity of Aqueous Solutions of NaCl and KCl at High Pressures. *Int. J. Thermophys.* **1994**, *15*, 401−413.
(6) Abdulagatov, I. M.; Magomedov, U. B. Thermal Conductivity of Aqueous $ZnCl_2$ Solutions at High Temperatures and High Pressures. *Ind. Eng. Chem. Res.* **1998**, *37*, 4883−4888.
(7) Abdulagatov, I. M.; Magomedov, U. B. Measurements of Thermal Conductivity of Aqueous LiCl and LiBr Solutions from 293 to 473 Pressures up to 100 MPa. *Ber. Bunsen−Ges. Phys. Chem.* **1997**, *101*, 708−711.
(8) Abdulagatov, I. M.; Magomedov, U. B. Thermal Conductivity of Aqueous $CdCl_2$ and $CdBr_2$ Solutions from 293 K to 473 K at High Pressures up to 100 MPa. *J. Chem. Eng. Data* **1997**, *42*, 1165−1169.
(9) Abdulagatov, I. M.; Magomedov, U. B. Measurements of the Thermal Conductivity of Aqueous $CoCl_2$ Solutions at Pressures up to 100 MPa by Parallel-Plate Apparatus. *J. Chem. Eng. Jpn.* **1999**, *32*, 465−471.
(10) Abdulagatov, I. M.; Magomedov, U. B. Effect of Temperature and Pressure on the Thermal Conductivity of Aqueous CaI_2 Solutions. *High Temp.−High Pressures* **2000**, *32*, 599−611.
(11) Abdulagatov, I. M.; Magomedov, U. B. Thermal Conductivity of Aqueous BaI_2 Solutions in the Temperature Range 293−473 and the Pressure Range 0.1−100 MPa. *Fluid Phase Equilib.* **2000**, *171*, 243−252.
(12) Abdulagatov, I. M.; Magomedov, U. B. Thermal Conductivity of Aqueous KI and KBr Solutions at High Temperatures and High Pressures. *J. Solution Chem.* **2001**, *30*, 223−235.
(13) Abdulagatov, I. M.; Magomedov, U. B. Thermal Conductivity of Pure Water and Aqueous $SrBr_2$ Solutions at High Temperatures and High Pressures. *High Temp.−High Pressures* **2004**. In press.
(14) Aseyev, G. G. *Electrolytes. Properties of Solutions. Methods for Calculation of Multicomponent Systems and Experimental Data on Thermal Conductivity and Surface Tension*; Begell-House Inc.: New York, 1998.
(15) Magomedov, U. B. Thermal Conductivity of Binary and Multicomponent Aqueous Solutions of Inorganic Substances at High Parameters of State. *Russ. High Temp.* **2001**, *39*, 221−226.
(16) Kestin, J.; Sengers, J. V.; Kamgar-Parsi, B.; Levelt Sengers, J. M. H.Thermophysical Properties of Fluid H_2O. *J. Phys. Chem. Ref. Data* **1984**, *13*, 175−189.
(17) Gershuni, G. Z. Thermal Convection in the Space Between Vertical Coaxial Cylinders. *Dokl. Akad. Nauk USSR* **1952**, *86*, 697−698.
(18) Healy, J.; de Groot, J. J.; Kestin, J. The Theory of the Transient Hot-Wire Method for Measuring Thermal Conductivity. *Phys. C* **1976**, *82*, 392−408.
(19) Menashe, J.; Wakeham, W. A. Effect of Absorption of Radiation on Thermal Conductivity Measurements by the Transient Hot-Wire Technique. *Int. J. Heat Mass Transfer* **1982**, *25*, 661−672.

(20) Nieto de Castro, C. A.; Li, S. F. Y.; Maitland, G. C.; Wakeham, W. A. Thermal Conductivity of Toluene in the Temperature Range 35−90 °C at Pressures up to 600 MPa. *Int. J. Thermophys.* **1983**, *4*, 311−327.
(21) Ramires, M. L. V.; Nieto de Castro, C. A.; Nagasaka, Y.; Nagashima, A.; Assael, M. J.; Wakeham, W. A. Standard Reference Data for the Thermal Conductivity of Water. *J. Phys. Chem. Ref. Data* **1995**, *24*, 1377−1381.
(22) Ramires, M. L. V.; Nieto de Castro, C. A.; Perkins, R. A.; Nagasaka, Y.; Nagashima, A.; Assael, M. J.; Wakeham, W. A. Reference Data for the Thermal Conductivity of Standard Liquid Toluene Over a Wide Range of Temperature. *J. Phys. Chem. Ref. Data* **2000**, *29*, 133−139.
(23) Lemmon, E. W.; McLinden, M. O.; Huber, M. L. NIST Standard Reference Database 23: Reference Fluid Thermodynamic and Transport Properties-REFPROP, Version 7.0, *National Institute of Standards and Technology, Standard Reference Data Program*, Gaithersburg, 2002.
(24) Mamedov, A. M.; Akhundov, T. S. *Thermodynamic Properties of Gases and Liquids. Aromatic Hydrocarbons*; GSSSD: Moscow, 1978; Vol. 5.
(25) El'darov, V. S. Thermal Conductivity of Aqueous Solutions of Nitrate Salts. *Russ. J. Phys. Chem.* **1986**, *60*, 603−605.
(26) Nikolaev, V. A. Thermal Conductivity of Aqueous NaCl, Na_2SO_4, and $MgSO_4$ Solutions in the Wide Range of Parameters of State. Ph.D. Thesis, Baku, Oil and Gas Academy, 1984.
(27) Nagasaka, Y.; Okada, H.; Suzuki, J.; Nagashima, A. Absolute Measurements of the Thermal Conductivity of Aqueous NaCl Solutions at Pressures up to 40 MPa. *Ber. Bunsen−Ges. Phys. Chem.* **1983**, *87*, 859−866.
(28) McLinden, M. O.; Klein, S. A.; Perkins, R. A. An Extended Corresponding States Model for the Thermal Conductivity of Refrigerants and Refrigerant Mixtures. *Int. J. Refrig.* **2000**, *23*, 43−63
(29) Takizawa, S.; Murata, H.; Nagashima, A. Measurement of the Thermal Conductivity of Liquids by Transient at Atmospheric Pressure. *Bulletin JSME* **1978**, *21*, 273−278.
(30) Venart, J. E. S.; Prasad, R. C. Thermal Conductivity of Water and Oleum. *J. Chem. Eng. Data* **1980**, *25*, 196−198.
(31) Alloush, A.; Gosney, W. B.; Wakeham, W. A. A Transient Hot-Wire Instrument for Thermal Conductivity Measurements in Electrically Conducting Liquids at Elevated temperatures. *Int. J. Thermophys.* **1982**, *3*, 225−235.
(32) Rastorguev, Yu. L.; Pugach, V. V. Experimental Study of the Thermal Conductivity of Water at High Pressures. *Teploenergetika* **1970**, *4*, 77.
(33) Grigor'ev, E. B. Thermal Conductivity of Binary and Ternary Aqueous Salt Solutions. Ph.D. Thesis, Makhachkala, IPG DSC RAS, 1995.
(34) DiGuilio, R. M.; Lee, R. J.; Jeter, S. M.; Teja, A. S. Properties of Lithium Bromide-Water Solutions at High Temperatures and Concentrations-I. Thermal Conductivity. *ASHRAE Trans.* **1990**, *96*, 702−708.
(35) Guseinov, G. G. Experimental Study of the Thermal Conductivity of Aqueous Orto-Phosphoric and Orto-Boric Acids in the Temperature Range Between 293 and 368 K and at Atmospheric Pressure. In *Thermophysical Properties of Pure Substances and Aqueous Electrolyte Solutions*; Dagestan Scientific Center of the RAS: Makhachkala, 1978; pp 51−55.
(36) Castelli, V. J.; Stanley, E. M. Thermal Conductivity of Distilled Water as Function of Pressure and Temperature. *J. Chem. Eng. Data* **1974**, *19*, 8−11.
(37) Assael, M. J.; Charitidou, E.; Georgiadis, G. P.; Wakehan, W. A. Absolute Measurement of the Thermal Conductivity of Electrically Conducting Liquids. *Ber. Bunsen−Ges. Phys. Chem.* **1988**, *92*, 627−631.
(38) Ziebland, H. The Thermal Conductivity of Toluene. New Determinations and an Appraisal of Recent Experimental Work. *Int. J. Heat Mass Transfer* **1961**, *2*, 273−279.
(39) Vargaftik, N. B.; Os'minin, Yu. P. Thermal Conductivity of Aqueous Salt, Acid, and Alkali Solutions. *Teploenergetika* **1956**, *7*, 15−16.
(40) Lawson, A. W.; Lowell, R.; Jain, A. L. Thermal Conductivity of Water at High Pressures. *J. Chem. Phys.* **1959**, *30*, 643−647.
(41) Gazdiev, M. A.; Rastorguev, Yu. L. Thermal Conductivity of Aqueous Di- and Three-Ethyleneglycol. *Russ. J. Phys. Chem.* **1971**, *45*, 692−693.
(42) Challoner, A. R.; Powell, R. W. Thermal Conductivities of Liquids: New Determinations for Seven Liquids and Appraisal of Existing Values. *Proc. R. Soc. London, Ser. A* **1956**, *238*, 90−106.
(43) Bach, J.; Grigull, U. Unsteady-State Measurements of the Thermal Conductivity with Optical Recording. *Wärme-und Stoffübertragung* **1970**, *3*, 44−57.
(44) Dix, M.; Wakeham, W. A.; Zalaf, M. Thermal Conductivity of Liquid Water at High Pressures. In: Thermal Conductivity-20. Hasselman, D. P. H., Thomas, J. R., Jr., Eds.; Plenum Press: New York and London, 1988; pp 185−192.
(45) Stupak, P. M.; Aizen, A. M.; Yampol'skii, N. G. Problem of the Thermal Conductivity Determination by the Coaxial Cylinders Methodol. *Russ. Phys. Eng. J.* **1970**, *19*, 74−78.
(46) Tufeu, R.; Le Neindre, B.; Johannin, P. C. R. Conductibilité Thermique de Quelques Liquides. *Hebd. Seances Acad. Sci., Ser. B* **1966**, *262*, 229−231.
(47) Yata, J.; Minamiyama, I.; Tashiro, M.; Muragishi, H. Thermal Conductivity of Water and Steam at High Temperatures and Pressures. *Bull. JSME* **1979**, *22*, 1220−1226.
(48) Ripoche, P.; Rolin, M. Détermination des Caractéristiques Physicochimiques des Solutions Aqueuses Concentrées D'hydroxyde de Potassium Jusqu'á 180 C. II. Les Capacités Calorifiques at la Conductivité Thermique. *Bull. Soci. Chim. Fr.* **1980**, *9−10*, 380−385.
(49) Dietz, F. J.; de Groot, J. J.; Franck, E. U. The Thermal Conductivity of Water to 250 °C and 350 MPa. *Ber. Bunsen−Ges. Phys. Chem.* **1981**, *85*, 1005−1009.
(50) Cherneyeva, L. I. Experimental Study of Thermal Conductivity of Water and Steam at High Temperatures and pressures. *Heat Transfer−Sov. Res.* **1971**, *3*, 1−8.
(51) Vargaftik, N. B.; Filippov, L. P.; Tarzimanov, A. A.; Tozkii, E. E. *Thermal Conductivity of Liquids and Gases*; GSSSD: Moscow, 1978.
(52) Le Neindre, B.; Bury, P.; Tufeu, R.; Vodar, B. Thermal Conductivity of Water and Heavy Water in the Liquid State up to 370 °C. *J. Chem. Eng. Data* **1976**, *21*, 265−274.
(53) Venart, J. E. S. The Thermal Conductivity of Water/Steam. *Adv. Thermophys. Prop. at Extreme Temp. and Press. Proc. 3th Symp. on Thermophys. Prop.*; ASME: NY, 1965; pp 237−245.
(54) Ramires, M. L.; Fareleira, J. M. N. A.; Nieto de Castro, C. A.; Dix, M.; Wakeham, W. A. The Thermal Conductivity of Toluene and Water. *Int. J. Thermophys.* **1993**, *14*, 1119−1129.
(55) Geller, V. Z.; Paramonov, I. A.; Tatavosov, G. D. Study of the Thermal Conductivity of Toluene and Experimental Estimation of the Radiative Heat Transfer. *Thermophysical Properties of Liquids*; Nauka: Moscow, 1973; pp 93−97.
(56) Rastorguev, Yu. L.; Geller, V. Z.; Ganiev, Yu. A. Thermal Conductivity Study of Toluene. *Thermpohysical Properties of Substances*; LTIKhP: Leningrad, 1969; pp 142−145.
(57) Davis, P. S.; Theeuwe, F.; Bearman, R. J.; Gordon, R. P. Non-Steady-State, Hot Wire, Thermal Conductivity Apparatus. *J. Chem. Phys.* **1971**, *55*, 4776−4783.
(58) Yamada, T.; Yaguchi, T.; Nagasaka, Y.; Nagashima, A. Thermal Conductivity of Toluene in the Temperature Range 193−453 K. *High Temp.−High Pressures* **1993**, *25*, 513−518.
(59) Chiquillo, A. *Measurements of the Relative Thermal Conductivity of Aqueous Salt Solutions with a Transient Hot-Wire Method*; Juris Druck + Verlag: Zurich, 1967.
(60) Riedel, L. The Heat Conductivity of Aqueous Solutions of Strong Electrolytes. *Chem. Eng. Technol.* **1951**, *23*, 59−64.

Received for review November 20, 2003. Accepted February 23, 2004.

JE0342466